IAEA 60 Years
Atoms for Peace and Development

The Abdus Salam International Centre for Theoretical Physics

Cement and Bitumen: Radiolysis Effects

Michael I. Ojovan

Nuclear Engineer, Department of Nuclear Energy, IAEA, Vienna

Assistant Professor (Visiting), The University of Sheffield, UK (staff member 2002-2011)

Cements

- Cementitious wasteforms
- Radiation effects

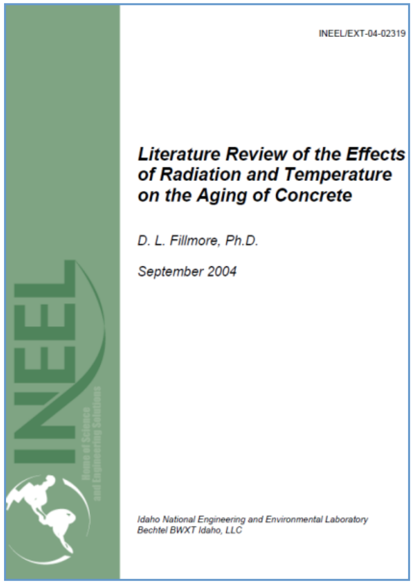

INEEL/EXT-04-02319

Literature Review of the Effects of Radiation and Temperature on the Aging of Concrete

D. L. Fillmore, Ph.D.

September 2004

Idaho National Engineering and Environmental Laboratory
Bechtel BWXT Idaho, LLC

The effects of low doses, $<10^{10}$ neutron/cm^2 or $<10^{10}$ Gy gamma, of radiation over periods of less than 50 years **do not seem to have a significant effect** on the concrete. Longer-term exposure, over 100 years, has not been studied.

Wikipedia: … very high fluxes are necessary to displace a sufficiently high number of atoms in the crystal lattice of minerals present in concrete before significant mechanical damage is observed. https://en.wikipedia.org/wiki/Concrete_degradation

Cementitious wasteforms

60 Years
IAEA
Atoms for Peace and Development

Five types of Portland cements (ASTM)

Cement type	Use
I	General purpose cement, when there are no extenuating conditions.
II	Aids in providing moderate resistance to sulphate attack
III	When high-early strength is required
IV	When a low heat of hydration is desired (in massive structures)
V	When high sulphate resistance is required

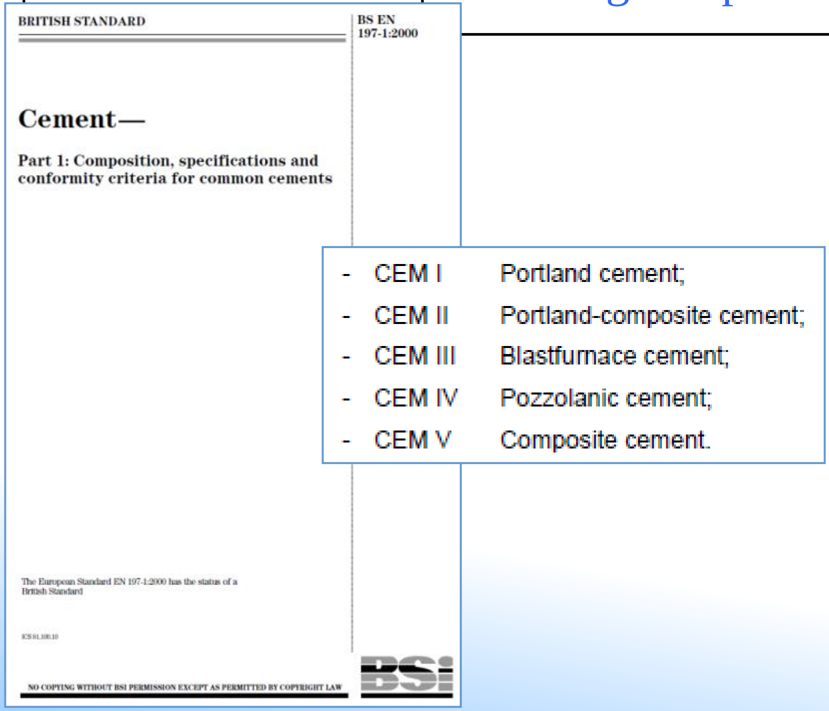

BRITISH STANDARD

BS EN
197-1:2000

Cement—

Part 1: Composition, specifications and conformity criteria for common cements

The European Standard EN 197-1:2000 has the status of a British Standard

ICS 91.100.10

NO COPYING WITHOUT BSI PERMISSION EXCEPT AS PERMITTED BY COPYRIGHT LAW

BSi

- CEM I	Portland cement;
- CEM II	Portland-composite cement;
- CEM III	Blastfurnace cement;
- CEM IV	Pozzolanic cement;
- CEM V	Composite cement.

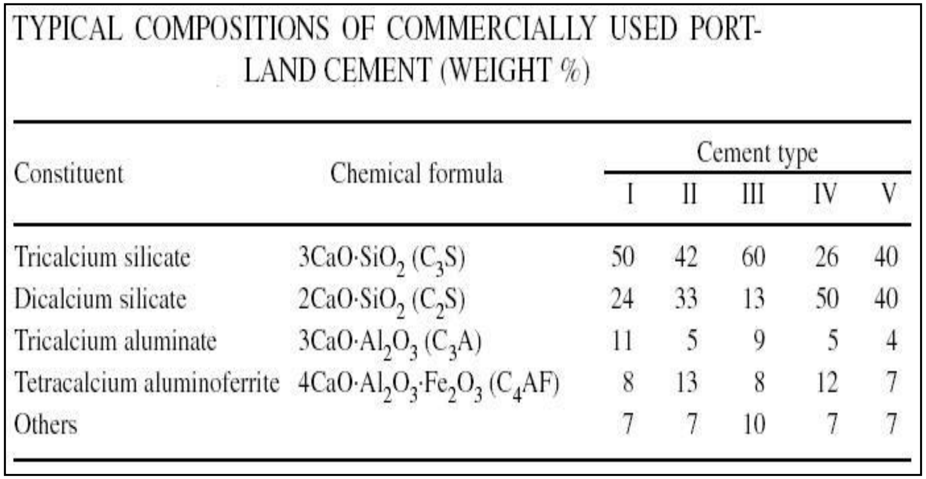

TYPICAL COMPOSITIONS OF COMMERCIALLY USED PORTLAND CEMENT (WEIGHT %)

Constituent	Chemical formula	Cement type I	II	III	IV	V
Tricalcium silicate	$3CaO \cdot SiO_2$ (C_3S)	50	42	60	26	40
Dicalcium silicate	$2CaO \cdot SiO_2$ (C_2S)	24	33	13	50	40
Tricalcium aluminate	$3CaO \cdot Al_2O_3$ (C_3A)	11	5	9	5	4
Tetracalcium aluminoferrite	$4CaO \cdot Al_2O_3 \cdot Fe_2O_3$ (C_4AF)	8	13	8	12	7
Others		7	7	10	7	7

Calcium silicates **C_3S** and C_2S that constitute about 75% of a Portland cement by weight react with water to produce two new compounds: calcium hydroxide and a calcium silicate hydrate called tobermorite gel.

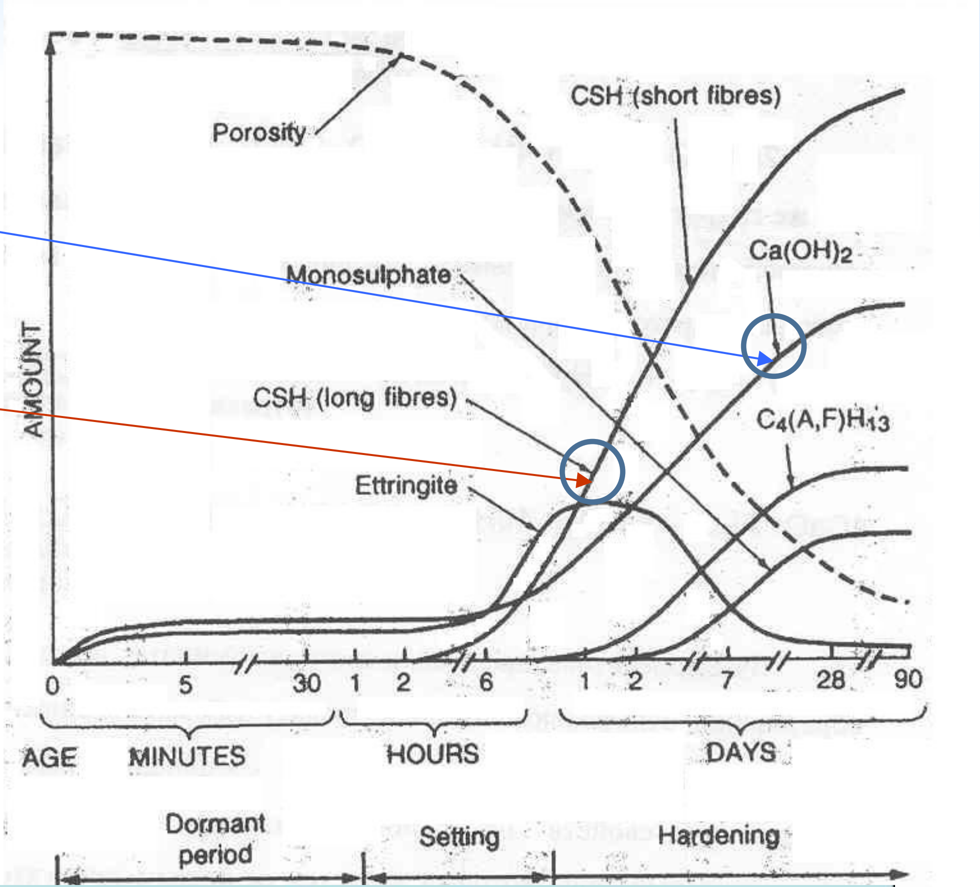

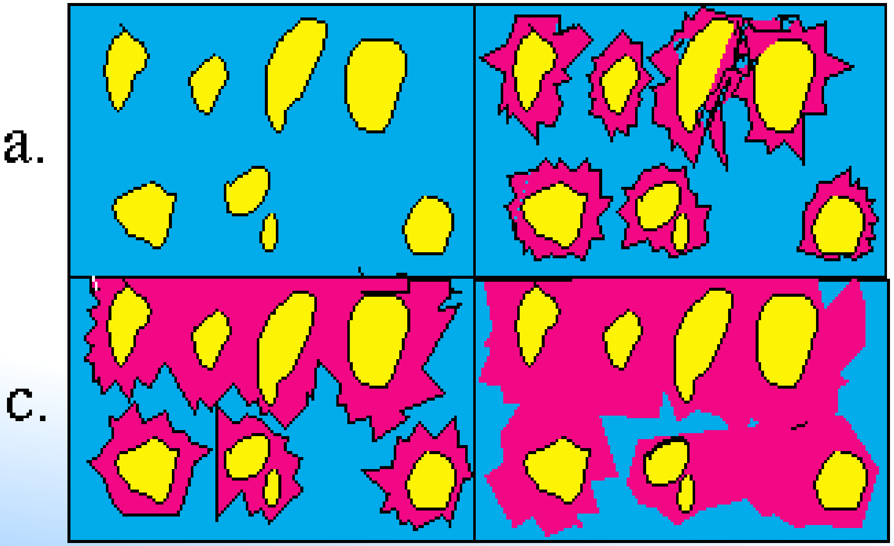

TRICALCIUM SILICATE

$$6CaO.2SiO_2 + 6H_2O = 3CaO.2SiO_2.3H_2O + 3Ca(OH)_2$$

Heat Liberated = - 114 kJ/mole

DICALCIUM SILICATE

$$4CaO.2SiO_2 + 4H_2O = 3CaO.2SiO_2.3H_2O + Ca(OH)_2$$

Heat Liberated = - 43 kJ/mole

Phase composition of hydrated cements

Phase	**Description**	**Notation**
	Crystalline	
Ettringite	$[Ca_3Al(OH)_6$ $12H_2O]_2(SO_4)_3$ $2H_2O$	AF_t
Monosulphate	$[Ca_2Al(OH)_6$ $6H_2O]_2(OH), (0.5SO_4)]_2$	AF_m
Hydrogarnet	$Ca_3Al_2(OH)_{12}$ – $Ca_3Al_2Si(OH)_8$	C_3AH_6 – C_3ASH_4
Portlandite	$Ca(OH)_2$	CH
	Amorphous	
Calcium silicate hydro-gel	Molar ration Ca/Si 1.7 ± 0.1	**C-S-H**

Development of the internal structure of hydrated cement occurs also after the concrete has set and continues for months (and even years) after placement. OPC will be hydrated by 95-98% within 12 months.

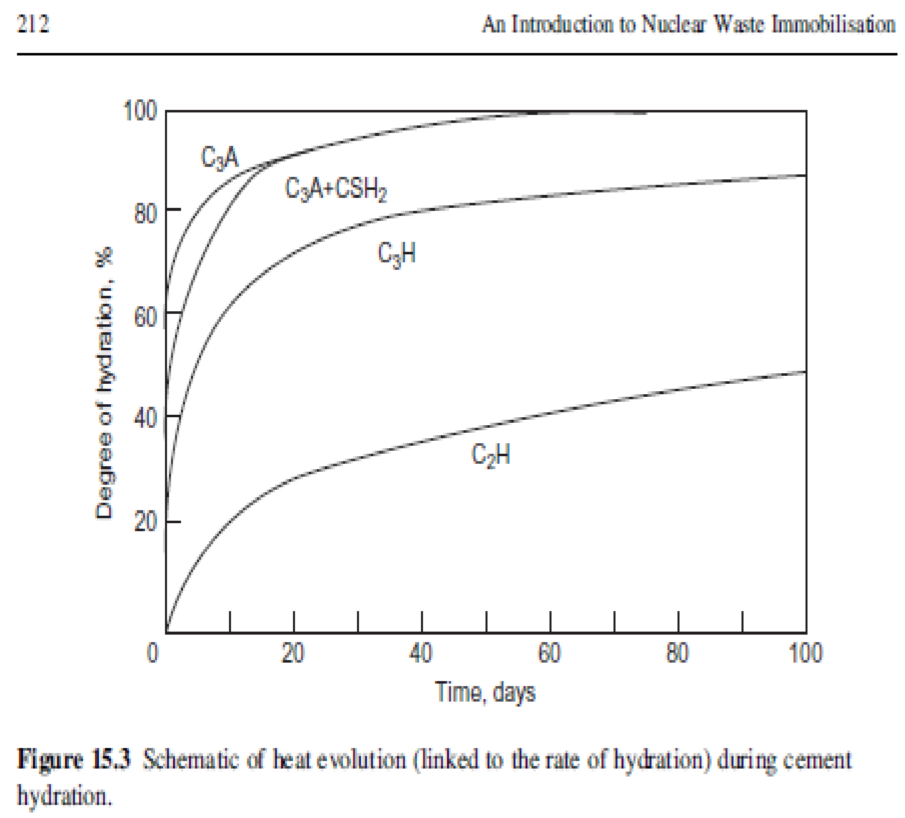

212 An Introduction to Nuclear Waste Immobilisation

Figure 15.3 Schematic of heat evolution (linked to the rate of hydration) during cement hydration.

After 12 months a typical Portland cement comprises an aqueous phase, which is largely confined to filling pores less than 1μ in radius and a paste matrix, which is itself heterogeneous.

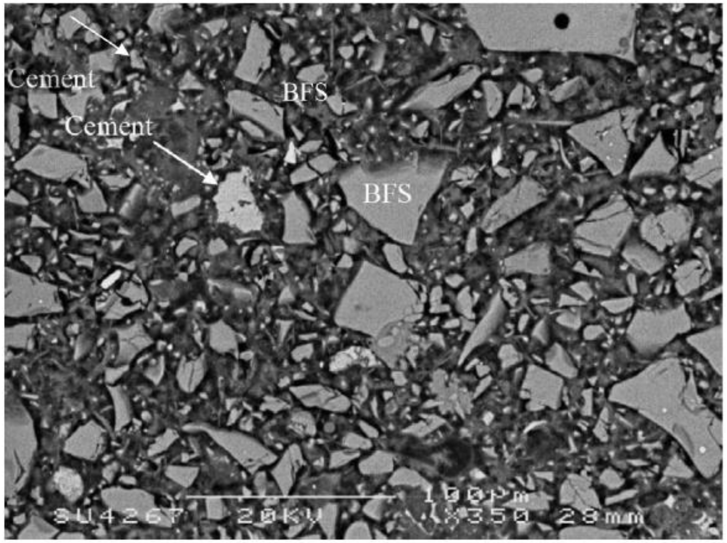

Figure 15.7 SEM image of 9:1 BFS:OPC cement, *w:c* 0.33 cured at 20°C for 90 days. *Sourc*
ISL U

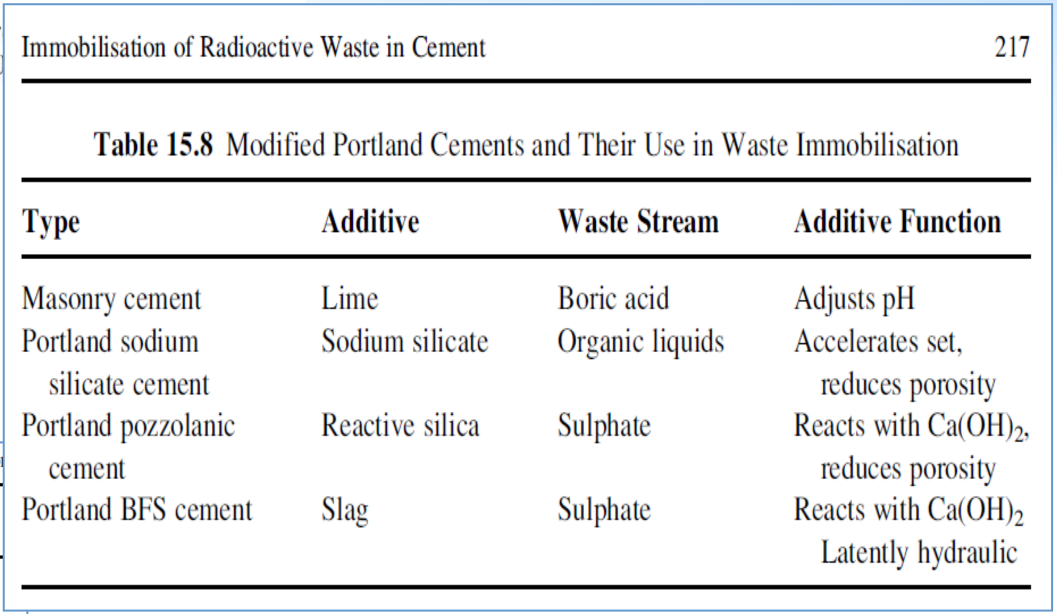

Table 15.8 Modified Portland Cements and Their Use in Waste Immobilisation

Type	Additive	Waste Stream	Additive Function
Masonry cement	Lime	Boric acid	Adjusts pH
Portland sodium silicate cement	Sodium silicate	Organic liquids	Accelerates set, reduces porosity
Portland pozzolanic cement	Reactive silica	Sulphate	Reacts with $Ca(OH)_2$, reduces porosity
Portland BFS cement	Slag	Sulphate	Reacts with $Ca(OH)_2$ Latently hydraulic

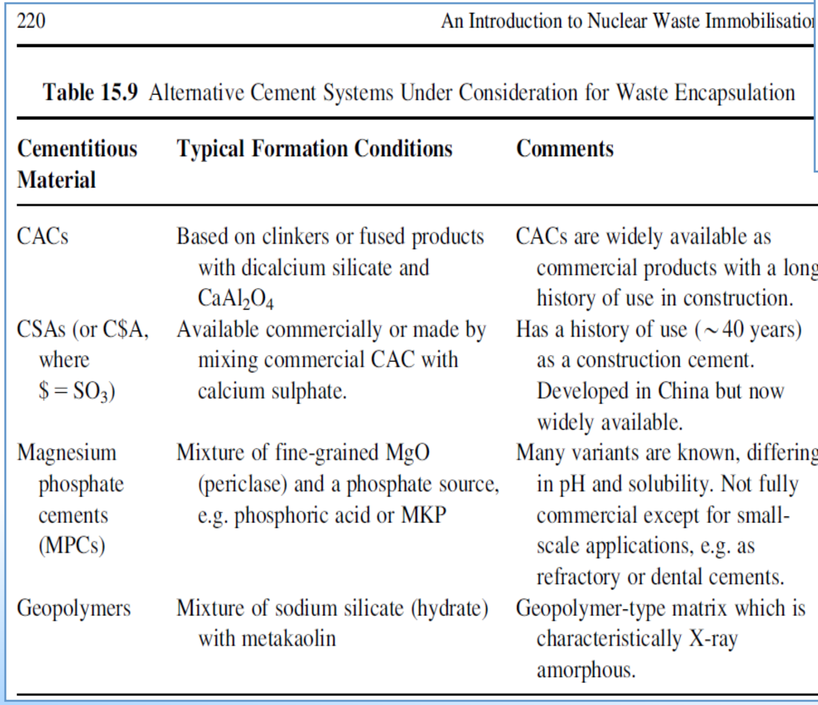

Table 15.9 Alternative Cement Systems Under Consideration for Waste Encapsulation

Cementitious Material	Typical Formation Conditions	Comments
CACs	Based on clinkers or fused products with dicalcium silicate and $CaAl_2O_4$	CACs are widely available as commercial products with a long history of use in construction.
CSAs (or C$A, where $ = SO_3)	Available commercially or made by mixing commercial CAC with calcium sulphate.	Has a history of use (~40 years) as a construction cement. Developed in China but now widely available.
Magnesium phosphate cements (MPCs)	Mixture of fine-grained MgO (periclase) and a phosphate source, e.g. phosphoric acid or MKP	Many variants are known, differing in pH and solubility. Not fully commercial except for small-scale applications, e.g. as refractory or dental cements.
Geopolymers	Mixture of sodium silicate (hydrate) with metakaolin	Geopolymer-type matrix which is characteristically X-ray amorphous.

Pore Water + Solids: The most important is the tobermorite gel (CHS), which is the main cementing component of concrete. The remaining three phases are crystalline and correspond more closely to defined stoichiometry. Portlandite typically comprises 20-25% of the fully hydrated paste, whereas AFm and AFt phases comprise 5-10% of the paste.

Radiation effects in water

Ionizing radiation produces abundant **secondary electrons** that rapidly slow down (thermalize) to energies below 7.4 eV, the threshold to produce electronic transitions in liquid water. Depending on the amount of energy transferred to the electron, the molecule can undergo: • Ionization (threshold in water ~ 13 eV); • Excitation (threshold in water ~ 7.4 eV); • Thermal transfer. Direct ionization of water produces a **radical ion** and a free **subexcitation electron** (E < 7.4 eV).

$$H_2O \xrightarrow{rad} H_2O^{\cdot +} + e^{-}$$

Energy transfer can produce a water molecule in an **excited state.**

$$H_2O \xrightarrow{rad} H_2O^{*}$$

The time scale for the creation of these species is on the order of **10^{-16} s**. The **three initial species** begin to diffuse and react with each other or other molecules in the medium. Some of these reactions produce **radicals.** Radical refers to an atom or molecule that contains an unpaired electron. Radicals are highly reactive. Radicals can be neutral or charged.

The electron is captured by water through dipolar interactions, becoming solvated, or it can react with H^+ to form a radical:

$$e^- + H_2O \rightarrow e^-_{aq}$$

$$e^- + H^+ \rightarrow H\cdot$$

The radical ion of water can dissociate to produce a hydroxyl radical and a hydrogen ion.

$$H_2O\cdot^+ \rightarrow H^+ + HO\cdot$$

The excited water molecule can dissipate excess energy by **bond breakage** to produce hydroxyl and hydrogen radicals (it takes ~ 5 eV to break the O-H bond)

$$H_2O^* \rightarrow HO\cdot + H\cdot$$

Thus, the **three initial species** $H_2O^+\cdot$, H_2O^*, e^- react further to produce **chemically reactive species**: HO·, H·, and e_{aq}^-. These radicals are much more reactive than HO^- or H^+ from ionic dissociation.

After ~10^{-12} s the chemically reactive species are still located in the vicinity of the original H^2O^*, $H^2O\cdot^+$ and e^- species where they formed. As the diffusion proceeds species may come close enough together to **react with each other.** A variety of reactions are possible in the track of the charged particle.

$$HO\cdot + HO\cdot \rightarrow H_2O_2$$

$$HO\cdot + e^-_{aq} \rightarrow OH^-$$

$$HO\cdot + H\cdot \rightarrow H_2O$$

$$H^+ + e^-_{aq} \rightarrow H\cdot$$

$$e^-_{aq} + e^-_{aq} + 2\,H_2O \rightarrow H_2 + 2\,OH^-$$

$$e^-_{aq} + H\cdot + H_2O \rightarrow H_2 + OH^-$$

$$H\cdot + H\cdot \rightarrow H_2$$

Specie	**D,** (10^{-5} cm^2 s^{-1})	**R (Å)**
OH	2	2.4
e^-_{aq}	5	2.1
H_3O^+	8	0.30
H	8	0.42

Most of these reactions **remove** chemically reactive species from the system. With time (by ~ 10^{-6} s) all of the reactive species have diffused sufficiently far that further reactions are unlikely.

Radiation chemical yield is characterised by the G-value: the number of a particular species produced **per 100 ev** of energy loss.

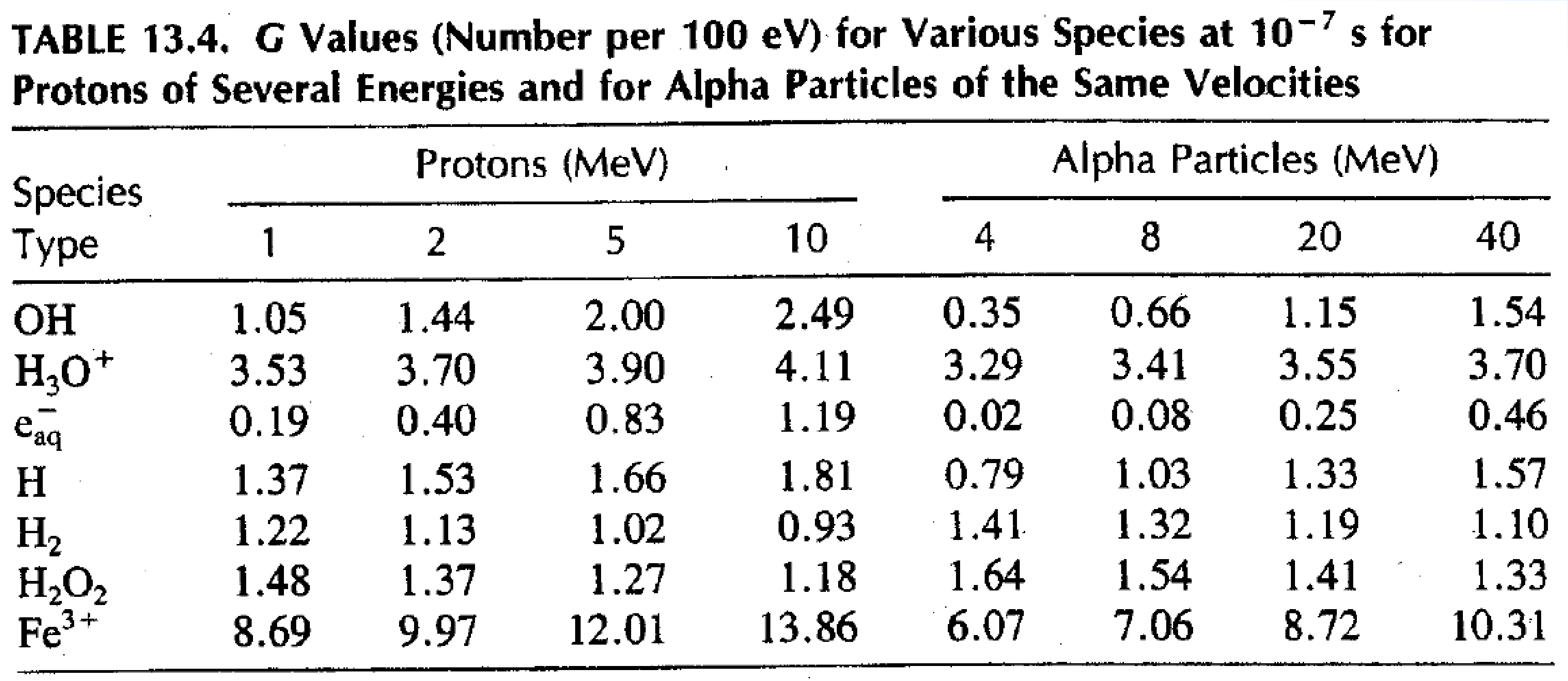

TABLE 13.4. G Values (Number per 100 eV) for Various Species at 10^{-7} s for Protons of Several Energies and for Alpha Particles of the Same Velocities

Species Type	Protons (MeV)				Alpha Particles (MeV)			
	1	2	5	10	4	8	20	40
OH	1.05	1.44	2.00	2.49	0.35	0.66	1.15	1.54
H_3O^+	3.53	3.70	3.90	4.11	3.29	3.41	3.55	3.70
e^-_{aq}	0.19	0.40	0.83	1.19	0.02	0.08	0.25	0.46
H	1.37	1.53	1.66	1.81	0.79	1.03	1.33	1.57
H_2	1.22	1.13	1.02	0.93	1.41	1.32	1.19	1.10
H_2O_2	1.48	1.37	1.27	1.18	1.64	1.54	1.41	1.33
Fe^{3+}	8.69	9.97	12.01	13.86	6.07	7.06	8.72	10.31

Radiation effects in cements

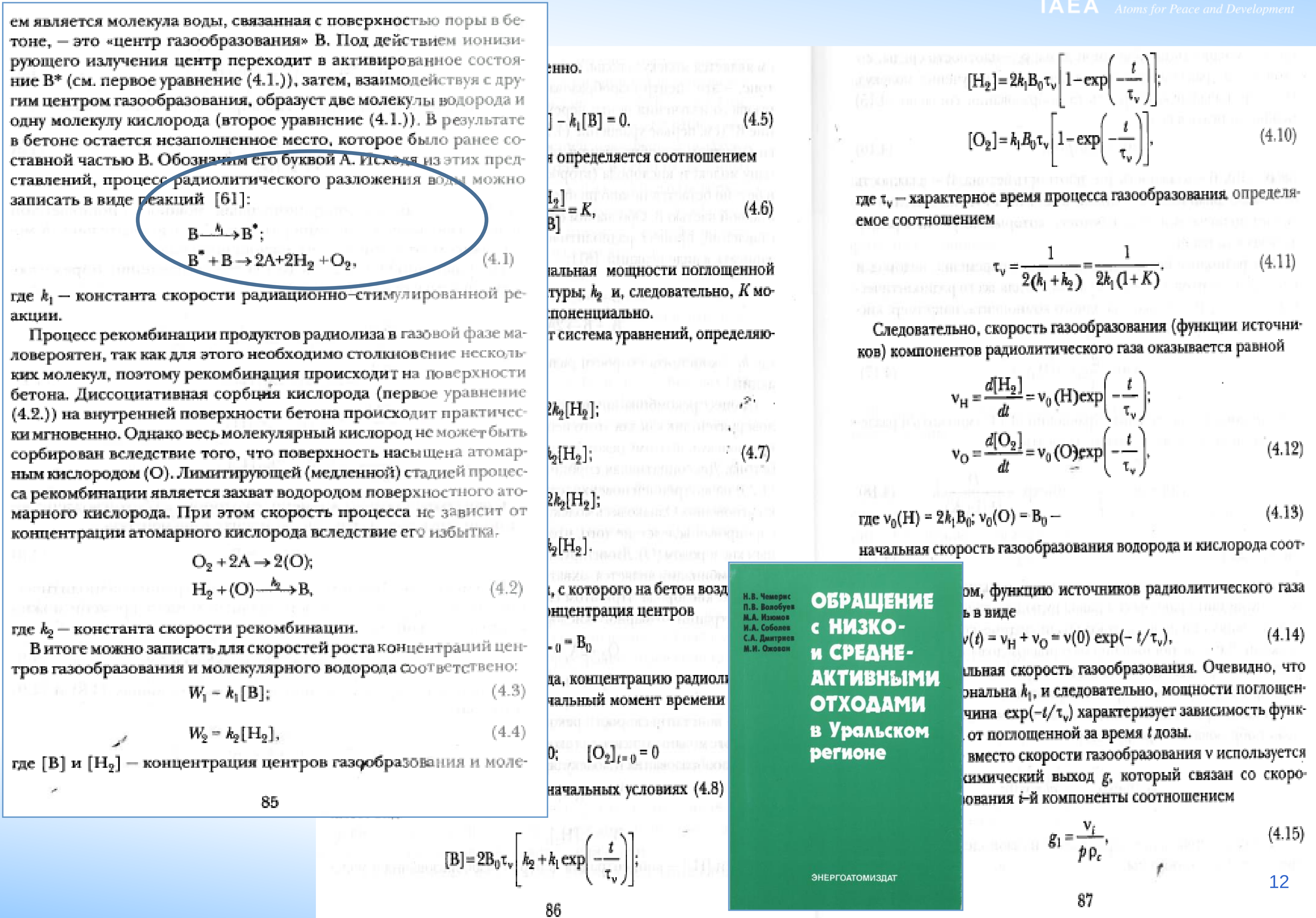

ем является молекула воды, связанная с поверхностью поры в бетоне, – это «центр газообразования» В. Под действием ионизирующего излучения центр переходит в активированное состояние В* (см. первое уравнение (4.1.)), затем, взаимодействуя с другим центром газообразования, образует две молекулы водорода и одну молекулу кислорода (второе уравнение (4.1.)). В результате в бетоне остается незаполненное место, которое было ранее составной частью В. Обозначим его буквой А. Исходя из этих представлений, процесс радиолитического разложения воды можно записать в виде реакций [61]:

$$\mathrm{B} \xrightarrow{k_1} \mathrm{B}^*;$$

$$\mathrm{B}^* + \mathrm{B} \rightarrow 2\mathrm{A} + 2\mathrm{H}_2 + \mathrm{O}_2, \qquad (4.1)$$

где k_1 – константа скорости радиационно-стимулированной реакции.

Процесс рекомбинации продуктов радиолиза в газовой фазе маловероятен, так как для этого необходимо столкновение нескольких молекул, поэтому рекомбинация происходит на поверхности бетона. Диссоциативная сорбция кислорода (первое уравнение (4.2.)) на внутренней поверхности бетона происходит практически мгновенно. Однако весь молекулярный кислород не может быть сорбирован вследствие того, что поверхность насыщена атомарным кислородом (О). Лимитирующей (медленной) стадией процесса рекомбинации является захват водородом поверхностного атомарного кислорода. При этом скорость процесса не зависит от концентрации атомарного кислорода вследствие его избытка.

$$\mathrm{O}_2 + 2\mathrm{A} \rightarrow 2(\mathrm{O});$$

$$\mathrm{H}_2 + (\mathrm{O}) \xrightarrow{k_2} \mathrm{B}, \qquad (4.2)$$

где k_2 – константа скорости рекомбинации.

В итоге можно записать для скоростей роста концентраций центров газообразования и молекулярного водорода соответствено:

$$W_1 = k_1[\mathrm{B}]; \qquad (4.3)$$

$$W_2 = k_2[\mathrm{H}_2], \qquad (4.4)$$

где [В] и $[\mathrm{H}_2]$ – концентрация центров газообразования и моле-

85

енно.

$$] - k_1[\mathrm{B}] = 0. \qquad (4.5)$$

я определяется соотношением

$$\frac{\mathrm{H}_2]}{\mathrm{B}]} = K, \qquad (4.6)$$

иальная мощности поглощенной
туры; k_2 и, следовательно, K мо-
споненциально.
т система уравнений, определяю-

$$2k_2[\mathrm{H}_2];$$

$$k_2[\mathrm{H}_2]; \qquad (4.7)$$

$$2k_2[\mathrm{H}_2];$$

$$k_2[\mathrm{H}_2].$$

, с которого на бетон возд
онцентрация центров

$$_{=0} = \mathrm{B}_0$$

да, концентрацию радиол
чальный момент времени

$$0; \qquad [\mathrm{O}_2]_{t=0} = 0$$

начальных условиях (4.8)

$$[\mathrm{B}] = 2\mathrm{B}_0\tau_v\left[k_2 + k_1\exp\left(-\frac{t}{\tau_v}\right)\right];$$

86

$$[\mathrm{H}_2] = 2k_1\mathrm{B}_0\tau_v\left[1 - \exp\left(-\frac{t}{\tau_v}\right)\right];$$

$$[\mathrm{O}_2] = k_1 B_0\tau_v\left[1 - \exp\left(-\frac{t}{\tau_v}\right)\right], \qquad (4.10)$$

где τ_v – характерное время процесса газообразования, определяемое соотношением

$$\tau_v = \frac{1}{2(k_1 + k_2)} = \frac{1}{2k_1(1+K)}. \qquad (4.11)$$

Следовательно, скорость газообразования (функции источников) компонентов радиолитического газа оказывается равной

$$v_\mathrm{H} = \frac{d[\mathrm{H}_2]}{dt} = v_0(\mathrm{H})\exp\left(-\frac{t}{\tau_v}\right);$$

$$v_\mathrm{O} = \frac{d[\mathrm{O}_2]}{dt} = v_0(\mathrm{O})\exp\left(-\frac{t}{\tau_v}\right), \qquad (4.12)$$

где $v_0(\mathrm{H}) = 2k_1\mathrm{B}_0$; $v_0(\mathrm{O}) = \mathrm{B}_0$ – (4.13)

начальная скорость газообразования водорода и кислорода соот-

ом, функцию источников радиолитического газа
ь в виде

$$v(t) = v_\mathrm{H} + v_\mathrm{O} = v(0)\exp(-t/\tau_v), \qquad (4.14)$$

льная скорость газообразования. Очевидно, что
ональна k_1, и следовательно, мощности поглощен-
чина $\exp(-t/\tau_v)$ характеризует зависимость функ-
от поглощенной за время t дозы.
вместо скорости газообразования v используется
химический выход g, который связан со скоро-
ования i-й компоненты соотношением

$$g_1 = \frac{v_i}{p\rho_c}, \qquad (4.15)$$

87

Н.В. Чемерис
П.В. Волобуев
М.А. Изюмов
И.А. Соболев
С.А. Дмитриев
М.И. Ожован

ОБРАЩЕНИЕ с НИЗКО- и СРЕДНЕ-АКТИВНЫМИ ОТХОДАМИ в Уральском регионе

ЭНЕРГОАТОМИЗДАТ


ОБРАЩЕНИЕ с НИЗКО- и СРЕДНЕ- АКТИВНЫМИ ОТХОДАМИ в Уральском регионе

ЭНЕРГОАТОМИЗДАТ

блока (бесконечно большой блок); стационарное газовыделение из блока.

Первый случай будет наблюдаться, если характерное время τ_D выхода газа из блока вследствие диффузии намного больше периода полураспада радионуклида $T_{1/2}$. При этом почти весь образующийся газ будет оставаться в блоке, и его концентрация будет максимальной. Во втором случае наоборот $\tau_D << T_{1/2}$, поэтому после достижения некоторой предельной концентрации, сколько газа будет образовываться, столько и будет выходить за пределы блока. Если бетонный блок велик, то можно считать, что на про-

газ оста-

к виду

(4.26)

ть в виде

(4.27)

ость ра-

(4.28)

дов с ис-

— энер-

ражение

(4.29)

газосо-

(4.30)

— абсо-

При стационарном газовыделении из блока уравнение (4.29) можно записать так

$$D_e \frac{d^2c}{dx^2}+\nu=0, \qquad (4.31)$$

Его решение при граничных условиях (4.25) имеет вид

$$c(x)=\frac{\nu}{2D_e}(lx-x^2). \qquad (4.32)$$

Отсюда максимальную концентрацию газа в блоке можно вычислить по формуле

$$c_{\max}=\frac{\nu l^2}{8D_e}. \qquad (4.33)$$

Измерения газовыделения из различных типов бетона показали, что 60–70% газа по объему составляет водород, 20–30% – кислород, до 10% – другие газы [62].

В табл. 4.1 приведены исходные данные для расчета параметров газовыделения в бетоне.

Таблица 4.1. Исходные данные для расчета параметров газовыделения в бетоне

D_v, Гр	D_e, м²/с	Q, отн.ед	$g_0(0)$, 1/Гр	W, отн.ед	K	$\rho_б$, кг/м³	T, K	τ_D (при l = 10 м), лет	τ_D (при l = 1 м), лет
$5 \cdot 10^8$	$4 \cdot 10^{-9}$	0,20	$2{,}6 \cdot 10^{16}$	0,10	2,0	3000	293	80,3	0,803

Величина τ_D – время, за которое концентрация газа в блоке с характерным размером l уменьшается в e раз.

В табл. 4.2 приведены результаты расчета начальной мощности поглощенной дозы $p(0)$, начального времени газовыделения $\tau_v(0)$ и начальной скорости газообразования $\nu(0)$ при гомогенном распределении различных радионуклидов в бетоне.

Из табл. 4.2 видно, что при удельной активности 1 Ки/м³ величина $\tau_v(0)$ на много порядков превосходит период полураспада и характерное время газовыделения τ_D. Это значит, что за все время распада, в частности ^{137}Cs, лишь небольшая часть из $\tau_v(0)\cdot\nu(0)$ центров газообразования превратится в радиолитический газ. Величи-

91

Начальная мощность дозы и скорость газообразования

Радионуклид	$T_{1/2}$, лет	A, Ки/м³	$p(0)$, 10^{-6}Гр/с	$k_β$	$E_β$, МэВ	$K_γ$	$E_γ$, МэВ	$\tau_v(0)$, 10^7 лет	$\tau_v(0)\cdot\nu(0)$, 10^{26}м$^{-3}$
^{137}Cs	30,0	1,0	1,31	0,07	0,514	0,95	0,66	3,6	1,2
^{60}Co	5,26	1,0	2,93	0,99	0,314	1,0	1,17	1,6	1,2
^{90}Sr	27,7	1,0	1,07	1,0	0,546	0,0	0,0	4,0	1,2
^{109}Cd	1,24	1,0	0,173	0,0	0,0	1,0	0,08	27,0	1,2
^{170}Tm	0,367	1,0	1,92	1,0	0,97	0,03	0,08	2,3	1,2
^{192}Ir	0,203	1,0	0,167	1,0	0,67	0,6	0,3	2,8	1,2

на $\nu(0)$ уменьшается при увеличении удельной активности.

В начальные периоды времени напряжение σ в центре блока с газовыделением всего в 3 раза меньше, чем в блоке без газовыделения (табл. 4.3). В блоке без учета газовыделения концентрация и напряжение стремятся к некоторому предельному значению, в блоке с газовыделением – к нулевому (рис. 4.3)

Как отмечалось, характерное время газообразования $\tau_v(0)$ уменьшается при увеличении начальной активности. При этом возрастает количество связанной влаги, превратившейся в радиолитический газ, и, соответственно, возрастают концентрация газа и напряжение в бетоне. Результаты соответствующих расчетов приведены в табл. 4.4, из которой видно, что напряжение, возникающее в бетоне, примерно за три периода полураспада прямо

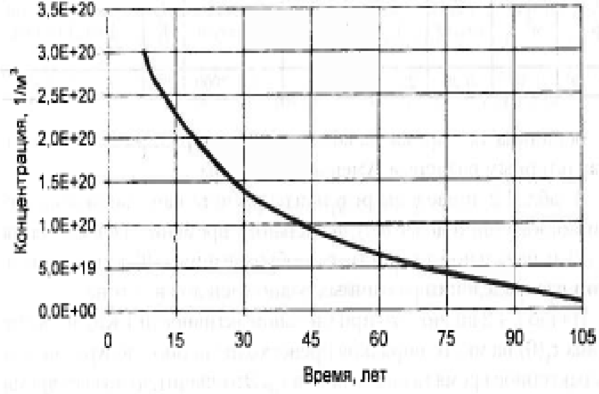

Рис. 4.3. Зависимость концентраций газа в центре блока от времени при свободном выходе газа из образца

92

Таблица 4.3. Зависимость от времени некоторых параметров газообразования для ^{137}Cs

Время t, лет	A, Ки/м³	p, 10^{-7}Гр/с	ν, 10^{18}м$^{-3}$с	σ, Па	$σ_{max}$, Па
0,0	1,0000	13,14	10,247	0	0
3,0	0,9330	12,26	9,560	0,758	0,242
6,0	0,8706	11,44	8,920	1,465	0,225
9,0	0,8706	11,44	8,920	1,465	0,225
12,0	0,7579	9,96	7,765	2,740	0,196
15,0	0,7071	9,29	7,245	3,314	0,183
18,0	0,6598	8,67	6,760	3,850	0,171
21,0	0,6156	8,09	6,308	4,350	0,159
24,0	0,5743	7,55	5,885	4,816	0,149
27,0	0,5359	7,04	5,491	5,251	0,139
30,0	0,5000	6,57	5,123	5,657	0,129
33,0	0,4665	6,13	4,780	6,036	0,121
36,0	0,4353	5,72	4,460	6,390	0,113
39,0	0,4061	5,34	4,161	6,719	0,105
42,0	0,3789	4,98	3,883	7,027	0,098
45,0	0,3536				
48,0	0,3299				
51,0	0,3078				
54,0	0,2872				
57,0	0,2679				
60,0	0,2500				
63,0	0,2333				
66,0	0,2176				
69,0	0,2031				
72,0	0,1985				
75,0	0,1768				
78,0	0,1649				
81,0	0,1539				
84,0	0,1436				
87,0	0,1340	1,76	1,373	9,799	0,035
90,0	0,1250	1,64	1,281	9,900	0,032
93,0	0,1166	1,53	1,195	9,995	0,030

93

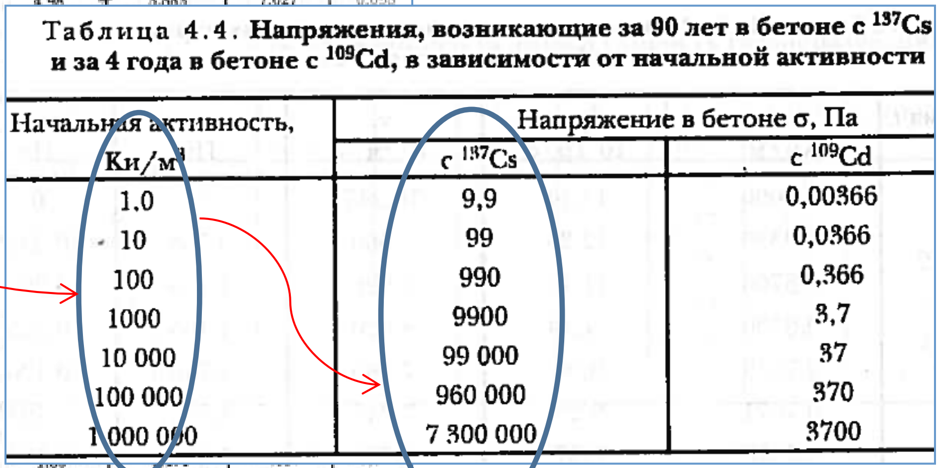

Таблица 4.4. Напряжения, возникающие за 90 лет в бетоне с ^{137}Cs и за 4 года в бетоне с ^{109}Cd, в зависимости от начальной активности

Начальная активность, Ки/м³	Напряжение в бетоне σ, Па	
	c ^{137}Cs	c ^{109}Cd
1,0	9,9	0,00366
10	99	0,0366
100	990	0,366
1000	9900	3,7
10 000	99 000	37
100 000	960 000	370
1 000 000	7 300 000	3700

ELSEVIER

Journal of Nuclear Materials 372 (2008) 1–15

www.elsevier.c

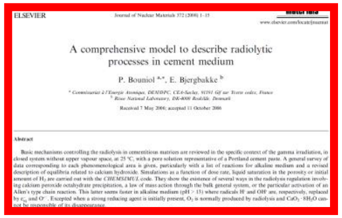

A comprehensive model to describe radiolytic processes in cement medium

P. Bouniol [a,*], E. Bjergbakke [b]

[a] *Commissariat à l'Energie Atomique, DEN/DPC, CEA-Saclay, 91191 Gif sur Yvette cedex, France*
[b] *Risoe National Laboratory, DK-4000 Roskilde, Denmark*

Received 7 May 2006; accepted 11 October 2006

Abstract

Basic mechanisms controlling the radiolysis in cementitious matrices are reviewed in the specific context of the gamm closed system without upper vapour space, at 25 °C, with a pore solution representative of a Portland cement paste. A g data corresponding to each phenomenological area is given, particularly with a list of reactions for alkaline mediur description of equilibria related to calcium hydroxide. Simulations as a function of dose rate, liquid saturation in the p amount of H_2 are carried out with the *CHEMSIMUL* code. They show the existence of several ways in the radiolysis re ing calcium peroxide octahydrate precipitation, a law of mass action through the bulk general system, or the particular Allen's type chain reaction. This latter seems faster in alkaline medium (pH > 13) where radicals $H^\cdot$ and $OH^\cdot$ are, respe by e^-_{aq} and $O^{\cdot -}$. Excepted when a strong reducing agent is initially present, O_2 is normally produced by radiolysis and C not be responsible of its disappearance.

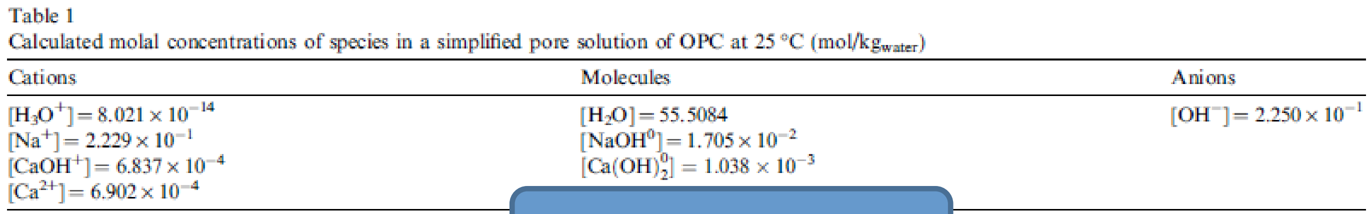

Table 1
Calculated molal concentrations of species in a simplified pore solution of OPC at 25 °C (mol/kg_{water})

Cations	Molecules	Anions
$[H_3O^+] = 8.021 \times 10^{-14}$ $[Na^+] = 2.229 \times 10^{-1}$ $[CaOH^+] = 6.837 \times 10^{-4}$ $[Ca^{2+}] = 6.902 \times 10^{-4}$	$[H_2O] = 55.5084$ $[NaOH^0] = 1.705 \times 10^{-2}$ $[Ca(OH)_2^0] = 1.038 \times 10^{-3}$	$[OH^-] = 2.250 \times 10^{-1}$

Pore solution

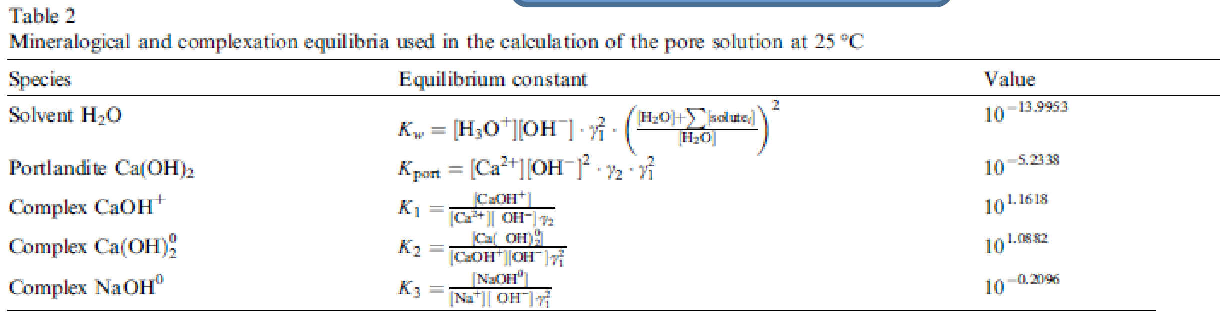

Table 2
Mineralogical and complexation equilibria used in the calculation of the pore solution at 25 °C

Species	Equilibrium constant	Value	Ref.
Solvent H_2O	$K_w = [H_3O^+][OH^-]\cdot\gamma_1^2\cdot\left(\frac{[H_2O]+\sum[solute_i]}{[H_2O]}\right)^2$	$10^{-13.9953}$	[3]
Portlandite $Ca(OH)_2$	$K_{port} = [Ca^{2+}][OH^-]^2\cdot\gamma_2\cdot\gamma_1^2$	$10^{-5.2338}$	This work
Complex $CaOH^+$	$K_1 = \frac{[CaOH^+]}{[Ca^{2+}][OH^-]\gamma_2}$	$10^{1.1618}$	---
Complex $Ca(OH)_2^0$	$K_2 = \frac{[Ca(OH)_2^0]}{[CaOH^+][OH^-]\gamma_1^2}$	$10^{1.0882}$	
Complex $NaOH^0$	$K_3 = \frac{[NaOH^0]}{[Na^+][OH^-]\gamma_1^2}$	$10^{-0.2096}$	

G values

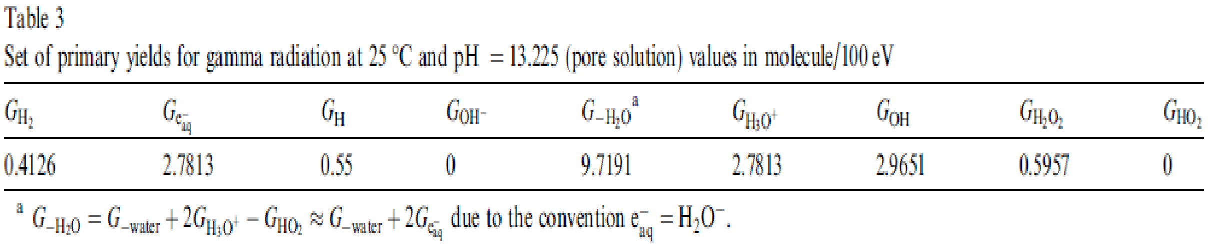

Table 3
Set of primary yields for gamma radiation at 25 °C and pH = 13.225 (pore solution) values in molecule/100 eV

G_{H_2}	$G_{e^-_{aq}}$	G_H	G_{OH^-}	G_{-H_2O} [a]	$G_{H_3O^+}$	G_{OH}	$G_{H_2O_2}$	G_{HO_2}
0.4126	2.7813	0.55	0	9.7191	2.7813	2.9651	0.5957	0

[a] $G_{-H_2O} = G_{-water} + 2G_{H_3O^+} - G_{HO_2} \approx G_{-water} + 2G_{e^-_{aq}}$ due to the convention $e^-_{aq} = H_2O^-$.

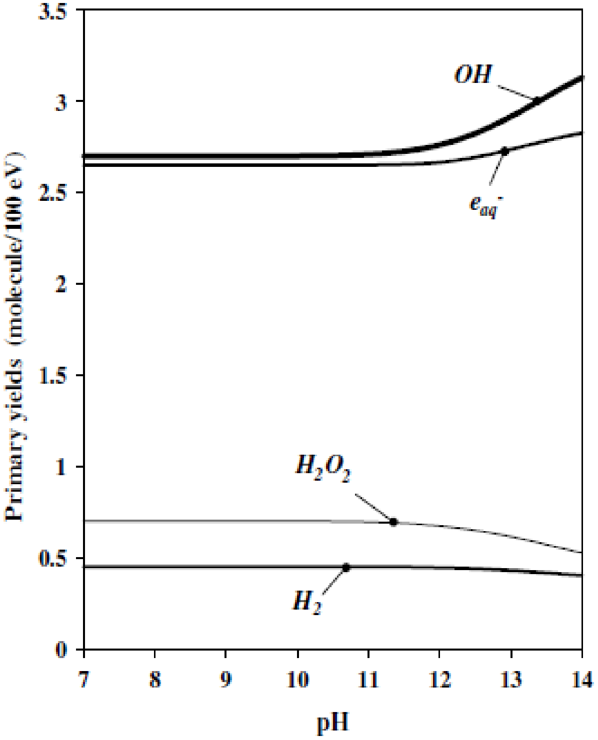

Fig. 1. Evolution of gamma primary yields for the main radiolytic species at 25 °C as a function of pH.

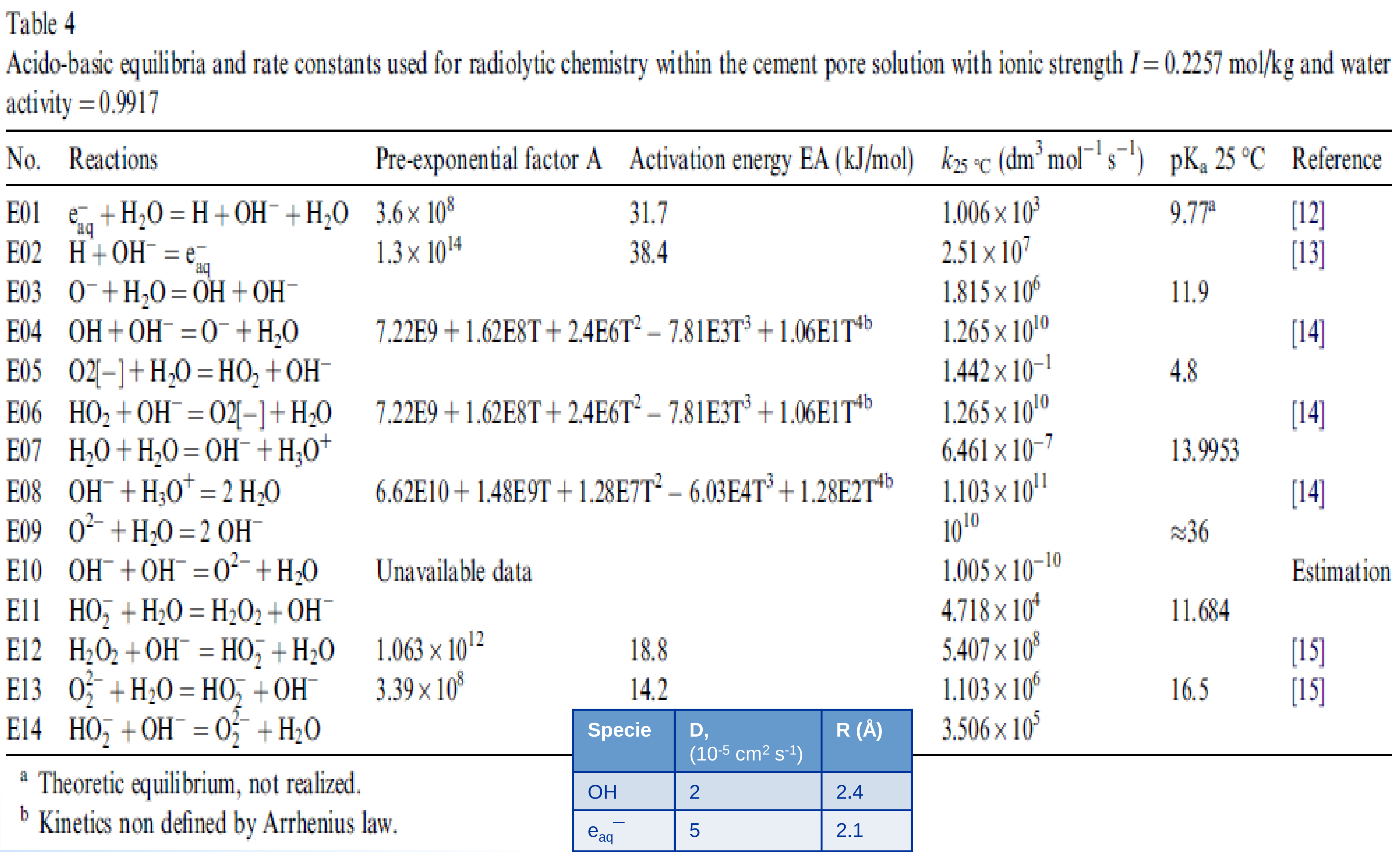

Table 4

Acido-basic equilibria and rate constants used for radiolytic chemistry within the cement pore solution with ionic strength $I = 0.2257$ mol/kg and water activity = 0.9917

No.	Reactions	Pre-exponential factor A	Activation energy EA (kJ/mol)	$k_{25\,°C}$ ($dm^3\,mol^{-1}\,s^{-1}$)	pK_a 25 °C	Reference
E01	$e^-_{aq} + H_2O = H + OH^- + H_2O$	3.6×10^8	31.7	1.006×10^3	9.77^a	[12]
E02	$H + OH^- = e^-_{aq}$	1.3×10^{14}	38.4	2.51×10^7		[13]
E03	$O^- + H_2O = OH + OH^-$			1.815×10^6	11.9	
E04	$OH + OH^- = O^- + H_2O$	$7.22E9 + 1.62E8T + 2.4E6T^2 - 7.81E3T^3 + 1.06E1T^{4b}$		1.265×10^{10}		[14]
E05	$O2[-] + H_2O = HO_2 + OH^-$			1.442×10^{-1}	4.8	
E06	$HO_2 + OH^- = O2[-] + H_2O$	$7.22E9 + 1.62E8T + 2.4E6T^2 - 7.81E3T^3 + 1.06E1T^{4b}$		1.265×10^{10}		[14]
E07	$H_2O + H_2O = OH^- + H_3O^+$			6.461×10^{-7}	13.9953	
E08	$OH^- + H_3O^+ = 2\,H_2O$	$6.62E10 + 1.48E9T + 1.28E7T^2 - 6.03E4T^3 + 1.28E2T^{4b}$		1.103×10^{11}		[14]
E09	$O^{2-} + H_2O = 2\,OH^-$			10^{10}	≈36	
E10	$OH^- + OH^- = O^{2-} + H_2O$	Unavailable data		1.005×10^{-10}		Estimation
E11	$HO_2^- + H_2O = H_2O_2 + OH^-$			4.718×10^4	11.684	
E12	$H_2O_2 + OH^- = HO_2^- + H_2O$	1.063×10^{12}	18.8	5.407×10^8		[15]
E13	$O_2^{2-} + H_2O = HO_2^- + OH^-$	3.39×10^8	14.2	1.103×10^6	16.5	[15]
E14	$HO_2^- + OH^- = O_2^{2-} + H_2O$			3.506×10^5		

[a] Theoretic equilibrium, not realized.

[b] Kinetics non defined by Arrhenius law.

Specie	D, (10^{-5} $cm^2\,s^{-1}$)	R (Å)
OH	2	2.4
e^-_{aq}	5	2.1
H_3O^+	8	0.30
H	8	0.42

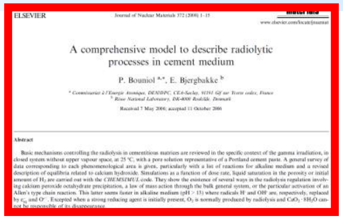

ELSEVIER Journal of Nuclear Materials 372 (2008) 1–15
www.elsevier.com/locate/jnucmat

A comprehensive model to describe radiolytic processes in cement medium

P. Bouniol [a,*], E. Bjergbakke [b]
[a] Commissariat à l'Energie Atomique, DEN/DPC, CEA-Saclay, 91191 Gif sur Yvette cedex, France
[b] Risø National Laboratory, DK-4000 Roskilde, Denmark

Received 7 May 2006; accepted 11 October 2006

Abstract

Basic mechanisms controlling the radiolysis in cementitious matrices are reviewed in the specific context of the gamma irradiation, in closed system without upper vapour space, at 25 °C, with a pore solution representative of a Portland cement paste. A general survey of data corresponding to each phenomenological area is given, particularly with a list of reactions for alkaline medium and a revised description of equilibria related to calcium hydroxide. Simulations as a function of dose rate, liquid saturation in the porosity or initial amount of H_2 are carried out with the *CHEMSIMUL* code. They show the existence of several ways in the radiolysis regulation involving calcium peroxide octahydrate precipitation, a law of mass action through the bulk general system, or the particular activation of an Allen's type chain reaction. This latter seems faster in alkaline medium (pH > 13) where radicals $H^•$ and $OH^•$ are, respectively, replaced by e^-_{aq} and $O^{•-}$. Excepted when a strong reducing agent is initially present, O_2 is normally produced by radiolysis and $CaO_2 \cdot 8H_2O$ cannot be responsible of its disappearance.

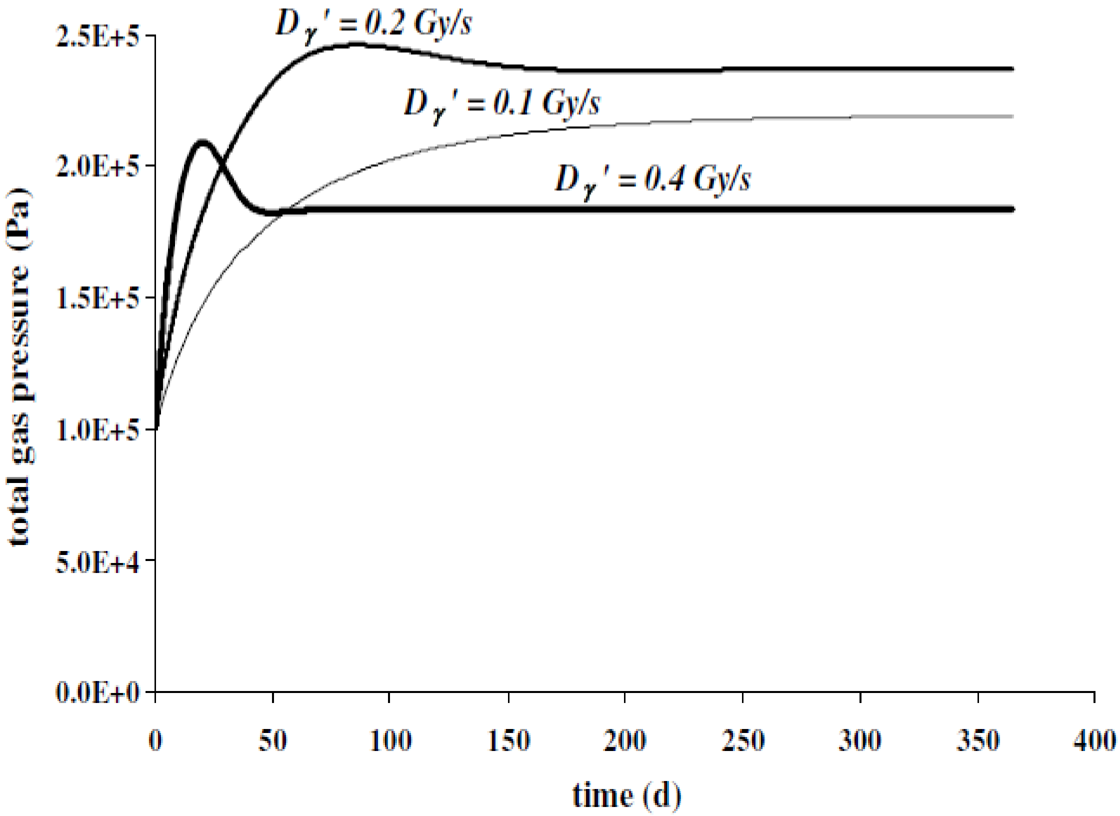

Fig. 8. Comparison of total gas pressures as a function of time in a confined cement matrix under gamma radiation at different dose rates for a liquid saturation degree of 0.75.

In conclusion, cementitious matrix exposed to gamma irradiation in closed system presents different regulating mechanisms able to limit radiolysis effects, or even to make this latter nondangerous (no important pressurization in the material). This behaviour cannot be extrapolated to open systems or alpha irradiation.

Journal of Hazardous Materials 187 (2011) 296–302

Contents lists available at ScienceDirect

Journal of Hazardous Materials

journal homepage: www.elsevier.com/locate/jhazmat

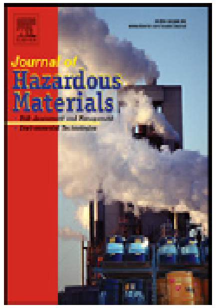

Long-term field and laboratory leaching tests of cemented radioactive wastes

Michael I. Ojovan[a,*], Galina A. Varlackova[b], Zoya I. Golubeva[b], Olga N. Burlaka[b]

[a] *Immobilisation Science Laboratory, Department of Materials Science and Engineering, University of Sheffield, Sir Robert Hadfield Building, Mappin Street, Sheffield S1 3JD, UK*
[b] *Scientific and Industrial Association 'Radon', 7-th Rostovsky Lane 2/14, Moscow, Russia*

ARTICLE INFO

Article history:
Received 15 November 2010
Received in revised form
24 December 2010
Accepted 5 January 2011
Available online 12 January 2011

Keywords:
Waste immobilisation
Cement
Leaching

ABSTRACT

Experiments with real and simulated radioactive cementitious wasteforms were set up to compare the leaching behaviour of cementitious wasteforms containing nuclear power plant operational waste in field and laboratory test conditions. Experiments revealed that the average annual ^{137}Cs leach rate in deionised water was about thirty-five times greater compared with the measured average value for the 1st year of the field test. Cumulative leached fraction of ^{137}Cs for 1st year (3.74%) was close to values reported in literature for similar laboratory experiments in deionised water, however more than two orders of magnitude higher than the 1st year leached fraction of ^{137}Cs in the repository test (0.01%). Therefore, to compare field and laboratory test results, a scaling factor is required in order to account for surface to volume factor difference, multiplied by a temperature factor and a leach rate decrease coefficient related to the ground water composition.

Journal of Hazardous Materials 187 (2011) 296–302

Contents lists available at ScienceDirect

Journal of Hazardous Materials

journal homepage: www.elsevier.com/locate/jhazmat

Long-term field and laboratory leaching tests of cemented radioactive wastes

Michael I. Ojovan[a,*], Galina A. Varlackova[b], Zoya I. Golubeva[a], Olga N. Burlaka[b]

ARTICLE INFO

Article history:
Received 15 November 2010
Received in revised form
24 December 2010
Accepted 5 January 2011
Available online 12 January 2011

Keywords:
Waste immobilisation
Cement
Leaching

ABSTRACT

Experiments with real and simulated radioactive cementitious wasteforms were set up to compare the leaching behaviour of cementitious wasteforms containing nuclear power plant operational waste in field and laboratory test conditions. Experiments revealed that the average annual ^{137}Cs leach rate in deionised water was about thirty-five times greater compared with the measured average value for the 1st year of the field test. Cumulative leached fraction of ^{137}Cs for 1st year (3.74%) was close to values reported in literature for similar laboratory experiments in deionised water, however more than two orders of magnitude higher than the 1st year leached fraction of ^{137}Cs in the repository test (0.01%). Therefore, to compare field and laboratory test results, a scaling factor is required in order to account for surface to volume factor difference, multiplied by a temperature factor and a leach rate decrease coefficient related to the ground water composition.

Fig. 1. Cementitious wasteforms after 12 years dwell in a near-surface testing repository.

Table 2
Radionuclide composition (in MBq/L) of radioactive waste.

^{137}Cs	^{134}Cs	^{60}Co	^{239}Pu	^{90}Sr	$\Sigma\beta^{a}$ (^{137}Cs)^{b}	$\Sigma\beta$(^{90}Sr + ^{90}Y)^{b}	$\Sigma\alpha$(^{239}Pu)^{b}
4.1	0.85	0.053	5.0×10^{-3}	1.5×10^{-4}	6.7	4.0	3.0×10^{-3}

[a] Σ stands for the sum of.
[b] Radionuclides given in brackets show the source radionuclides used for calibration.

Table 3
Characterization of wasteform samples used for long-term field tests.

Sample	Weight (kg)	Contact surface (cm^2)	Waste loading (wt.%)	Density (g/cm^3)	β_{tot}(^{90}Sr + ^{90}Y) (MBq/kg)	α_{tot}(^{239}Pu) (Bq/kg)
K-28	44.0[a]	5430	37.5	1.5	2.10	n.m.

[a] Total weight of three cylindrical samples (ø = h = 24 cm).

2.9. ^{60}Co irradiation tests

An additional factor which could affect leach rates from large-scale cement blocks is self-irradiation of samples due to natural decay of waste radionuclides [10,32]. The effects of irradiation were studied using non-radioactive cementitious wasteform samples after a hardening period of 1 year. Irradiation facility RHM-Gamma-20 was used with ^{60}Co sources. Cumulative dose used was 10^6 Gy for all samples irradiated which is expected to be not higher than the waste lifetime absorbed radiation dose. Dose rate applied was not inducing a significant temperature rise in the sample and the radiolysis hydrogen production rate was enough low and did not cause any damage of samples able to result in experimental artefacts.

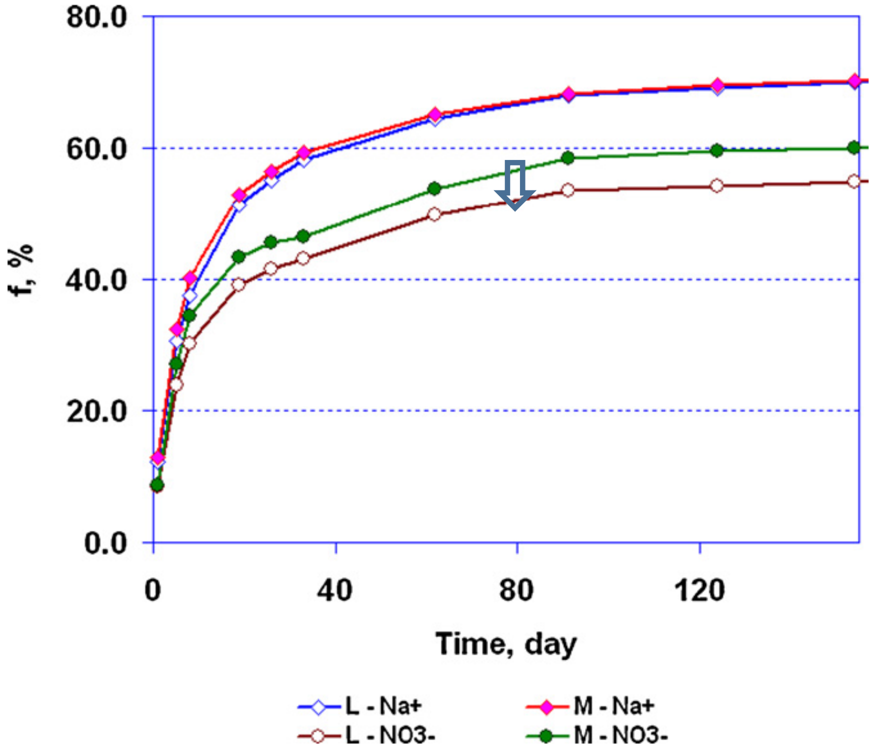

Fig. 5. Cumulative leached fractions of Na^+ and NO_3^- measured in the laboratory leach test of non-radioactive cementitious wasteform samples subjected (L) and not subjected (M) to ^{60}Co gamma irradiation. The cumulative dose was 10^6 Gy.

Gamma irradiation resistance of an early age slag-blended cement matrix for nuclear waste encapsulation

Neda Mobasher, Susan A. Bernal, and Hajime Kinoshita
Department of Materials Science & Engineering, Immobilisation Science Laboratory, The University of Sheffield, Sheffield S1 3JD, UK
Clint A. Sharrad
Research Centre for Radwaste and Decommissioning, Dalton Nuclear Institute, The University of Manchester, Manchester M13 9PL, UK
John L. Provis[a)]
Department of Materials Science & Engineering, Immobilisation Science Laboratory, The University of Sheffield, Sheffield S1 3JD, UK

- The crystalline phases were able to withstand the dose rate and total degree of gamma irradiation tested in the present study (4.77 MGy), without notable modifications.
- The Si and Al environments in the C–S–H type gel and secondary hydrate phases retained stability upon irradiation.
- Irradiation-induced carbonation, previously reported for PC-based systems, was not identified in the specimens.
- The reduced amount of $Ca(OH)_2$ in the system, owing to the small amount of PC used, appears to have minimized the formation of calcium peroxide octahydrate, which is an important intermediate in the radiation-induced carbonation process.

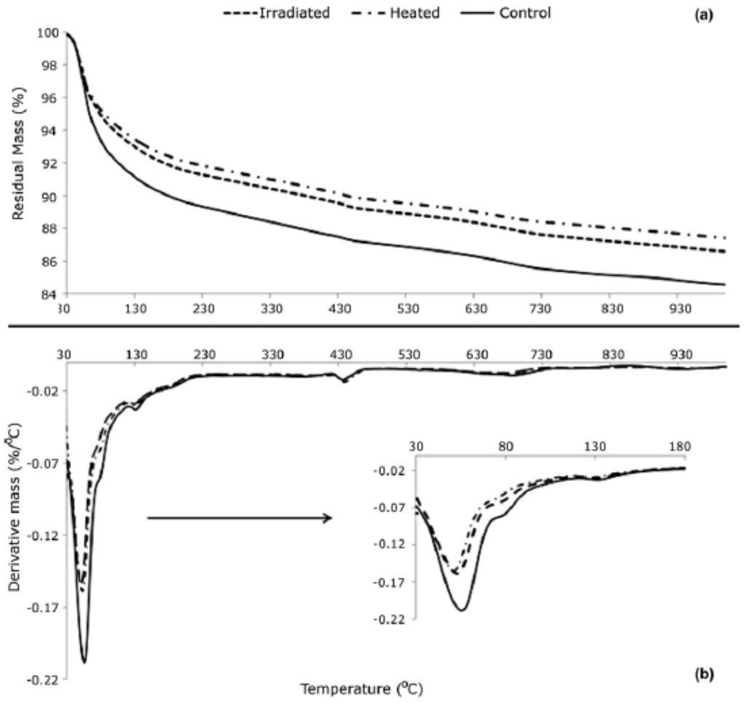

FIG. 4. Thermograms (A) and differential thermograms (B) (mass loss downwards) of the control, heated, and irradiated BFS:PC samples.

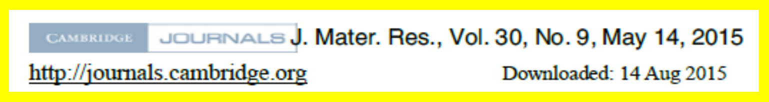

CAMBRIDGE JOURNALS J. Mater. Res., Vol. 30, No. 9, May 14, 2015
http://journals.cambridge.org

CAMBRIDGE JOURNALS J. Mater. Res., Vol. 30, No. 9, May 14, 2015
http://journals.cambridge.org

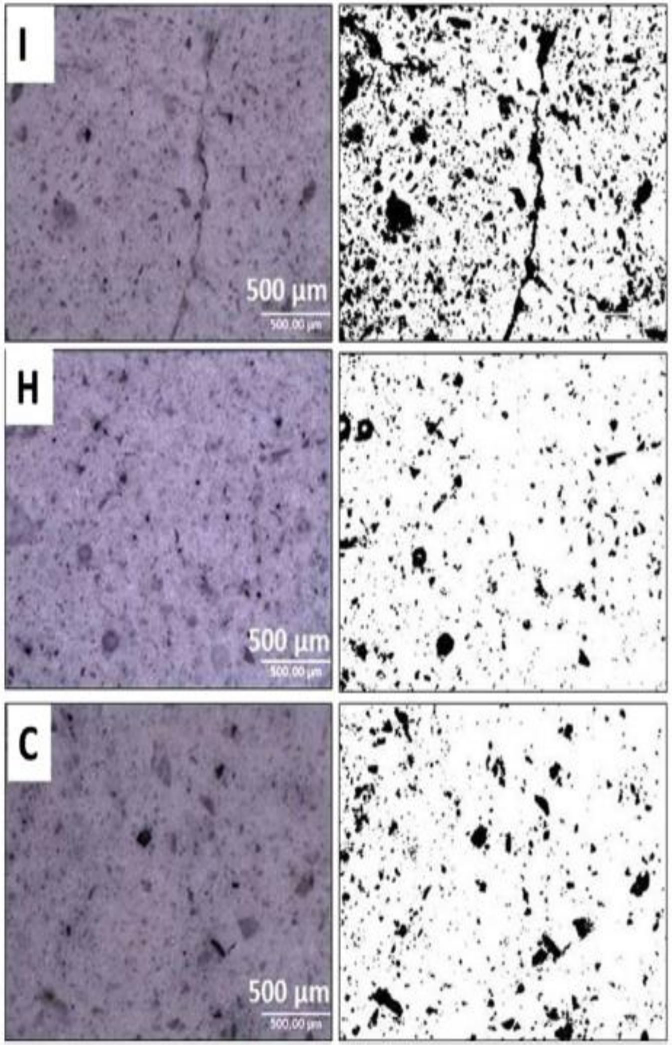

FIG. 5. Optical micrographs of (I) irradiated, (H) heated, and (C) control samples, and corresponding thresholded images regions.

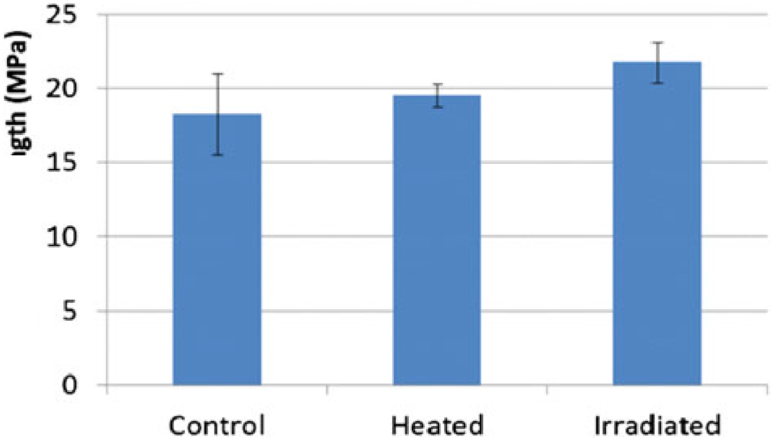

6. Compressive strength of BFS:PC pastes. Error bars show one lard deviation of three measurements.

This result demonstrates that the replacement of PC by BFS can modify the performance of the cement matrix under irradiation exposure. Gamma radiation caused a reduction in the content of physically bonded water within the binder, resulting in microcracking. Although exposure to 50 °C also caused a comparable level of water reduction in the grout, microcracks were not observed in that sample, which elucidates that the elevated temperature in the radiation chamber is not the main cause of the microcracks. The dehydration mechanisms in these two environments appear to be different, resulting in the different microstructures. Gamma irradiation also increased the compressive strength of the cement despite the increased porosity and microcracks, which may be due to enhancements in curing and/or the densification of the material.

Conclusions on cements

- Radiation durability of cements is high, at least 1 MGy by typical wasteform requirements. Cementitious matrix exposed to gamma irradiation in closed system presents different regulating mechanisms able to limit radiolysis effects with no important pressurization in the material.
- The slag cement-based grout withstands a gamma irradiation dose of 4.77 MGy over 256 h without reduction in its compressive strength.
- No significant differences can be seen in the leaching behaviour of irradiated samples and the leaching rates at the late stage are essentially the same for both irradiated and non irradiated samples.

References:

1. P. Bouniol, E. Bjergbakke. A comprehensive model to describe radiolytic processes in cement medium. *J. Nucl. Mater.*, **372**, 1–15 (2008).
2. N. Mobasher, S. A. Bernal, H. Kinoshita, C. A. Sharrad, J.L. Provis. Gamma irradiation resistance of an early age slag-blended cement matrix for nuclear waste encapsulation. J. Mater. Res., **30**, 1563-1571 (2015).
3. M.I. Ojovan, W.E. Lee. An Introduction to Nuclear Waste Immobilisation, 2nd Edition, Elsevier, Amsterdam, 362 p. (2014).
4. M.I. Ojovan, G.A. Varlackova, Z.I. Golubeva, O.N. Burlaka. Long-term field and laboratory leaching tests of cemented radioactive wastes. *J. Hazard. Mater.*, **187**, 296-302 (2011) .
5. D. L. Fillmore. Literature Review of the Effects of Radiation and Temperature on the Aging of Concrete. NEEL/EXT-04-02319, Idaho National Engineering and Environmental Laboratory Idaho Falls, Idaho 83415 (2004).
6. C. E. Acevedo, M. G. Serrato. Determining the Effects of Radiation on Aging Concrete Structures of Nuclear Reactors. Proc WM2010 Conference, March 7-11, 2010, Phoenix, AZ, Paper 10243 (2010).
7. R.O. Abdel Rahman, R.Z. Rahimov, N.R. Rahimova, M.I. Ojovan. Cementitious materials for nuclear waste immobilisation. 258 pages, Wiley, Chichester (2015).

Bitumen

- Bituminous wasteforms
- Radiation effects

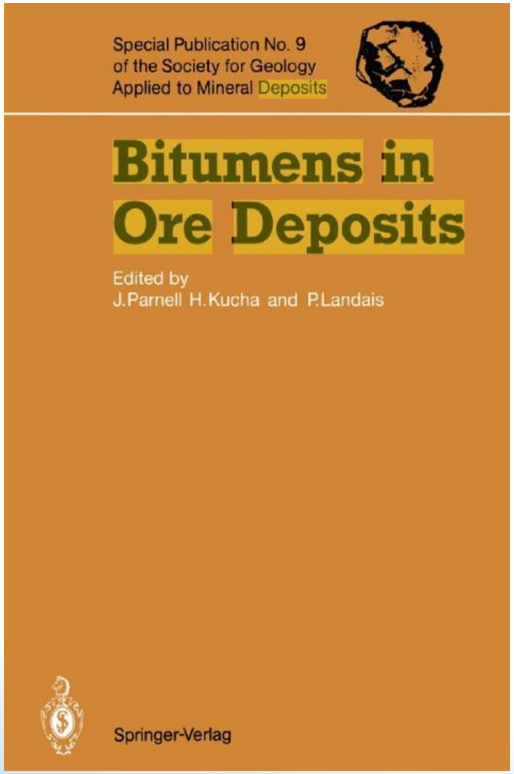

Special Publication No. 9
of the Society for Geology
Applied to Mineral Deposits

Bitumens in Ore Deposits

Edited by
J. Parnell H. Kucha and P. Landais

Springer-Verlag

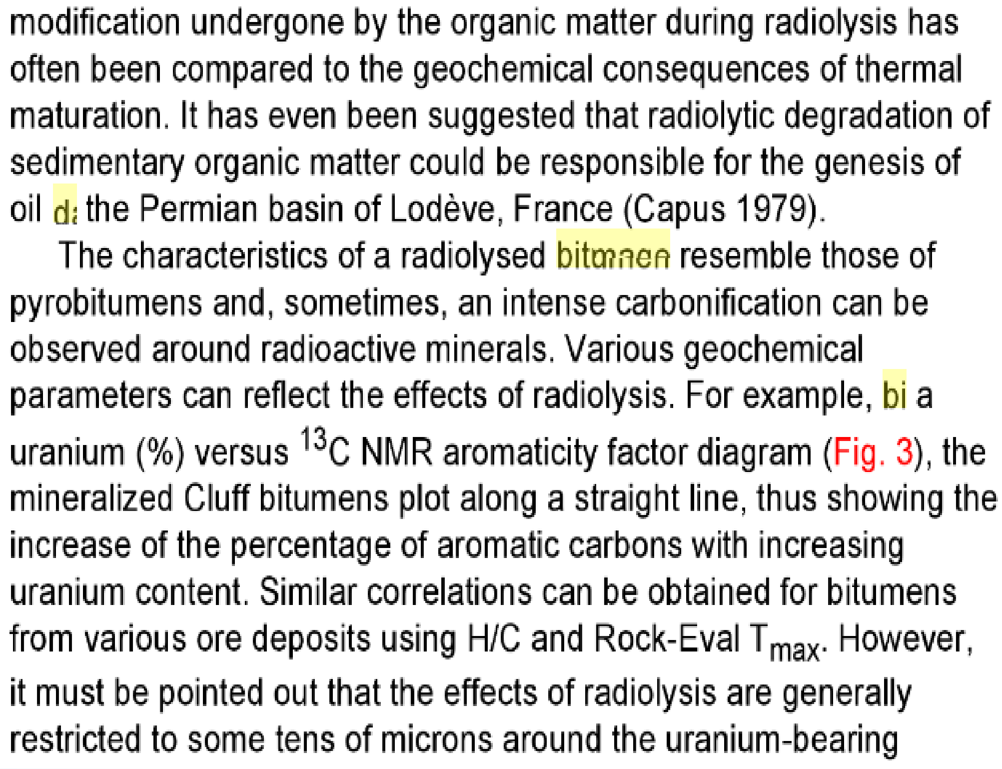

modification undergone by the organic matter during radiolysis has often been compared to the geochemical consequences of thermal maturation. It has even been suggested that radiolytic degradation of sedimentary organic matter could be responsible for the genesis of oil d the Permian basin of Lodève, France (Capus 1979).

The characteristics of a radiolysed bitumen resemble those of pyrobitumens and, sometimes, an intense carbonification can be observed around radioactive minerals. Various geochemical parameters can reflect the effects of radiolysis. For example, bi a uranium (%) versus ^{13}C NMR aromaticity factor diagram (Fig. 3), the mineralized Cluff bitumens plot along a straight line, thus showing the increase of the percentage of aromatic carbons with increasing uranium content. Similar correlations can be obtained for bitumens from various ore deposits using H/C and Rock-Eval T_{max}. However, it must be pointed out that the effects of radiolysis are generally restricted to some tens of microns around the uranium-bearing

Bituminous wasteforms

Bituminisation of radioactive waste is used for more than 50 years the total volume of radioactive waste immobilised by bitumen exceeding 200,000 m^3. Retention properties of bitumen are better than that of cements.

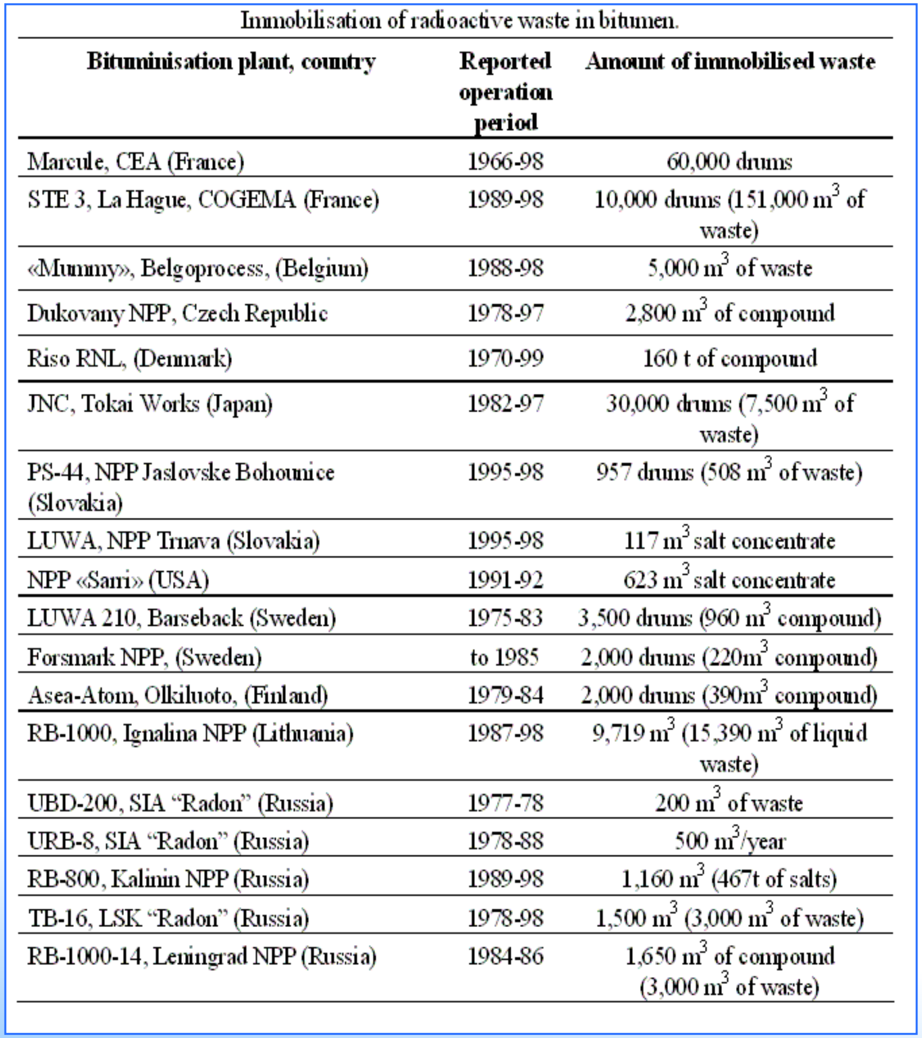

Immobilisation of radioactive waste in bitumen.

Bituminisation plant, country	Reported operation period	Amount of immobilised waste
Marcule, CEA (France)	1966-98	60,000 drums
STE 3, La Hague, COGEMA (France)	1989-98	10,000 drums (151,000 m^3 of waste)
«Mummy», Belgoprocess, (Belgium)	1988-98	5,000 m^3 of waste
Dukovany NPP, Czech Republic	1978-97	2,800 m^3 of compound
Riso RNL, (Denmark)	1970-99	160 t of compound
JNC, Tokai Works (Japan)	1982-97	30,000 drums (7,500 m^3 of waste)
PS-44, NPP Jaslovske Bohounice (Slovakia)	1995-98	957 drums (508 m^3 of waste)
LUWA, NPP Trnava (Slovakia)	1995-98	117 m^3 salt concentrate
NPP «Sarri» (USA)	1991-92	623 m^3 salt concentrate
LUWA 210, Barseback (Sweden)	1975-83	3,500 drums (960 m^3 compound)
Forsmark NPP, (Sweden)	to 1985	2,000 drums (220m^3 compound)
Asea-Atom, Olkiluoto, (Finland)	1979-84	2,000 drums (390m^3 compound)
RB-1000, Ignalina NPP (Lithuania)	1987-98	9,719 m^3 (15,390 m^3 of liquid waste)
UBD-200, SIA "Radon" (Russia)	1977-78	200 m^3 of waste
URB-8, SIA "Radon" (Russia)	1978-88	500 m^3/year
RB-800, Kalinin NPP (Russia)	1989-98	1,160 m^3 (467t of salts)
TB-16, LSK "Radon" (Russia)	1978-98	1,500 m^3 (3,000 m^3 of waste)
RB-1000-14, Leningrad NPP (Russia)	1984-86	1,650 m^3 of compound (3,000 m^3 of waste)

Bitumenization plant for radioactive waste from NPP Dukovany.

Advantages of a bitumen matrix are:

- **Water insolubility;**
- **Low diffusion of water;**
- **Chemical inertness;**
- **Plasticity and good rheological properties;**
- **Slow ageing rates;**
- **High incorporation capacity enabling high waste loadings;**
- **Readily available and low cost.**

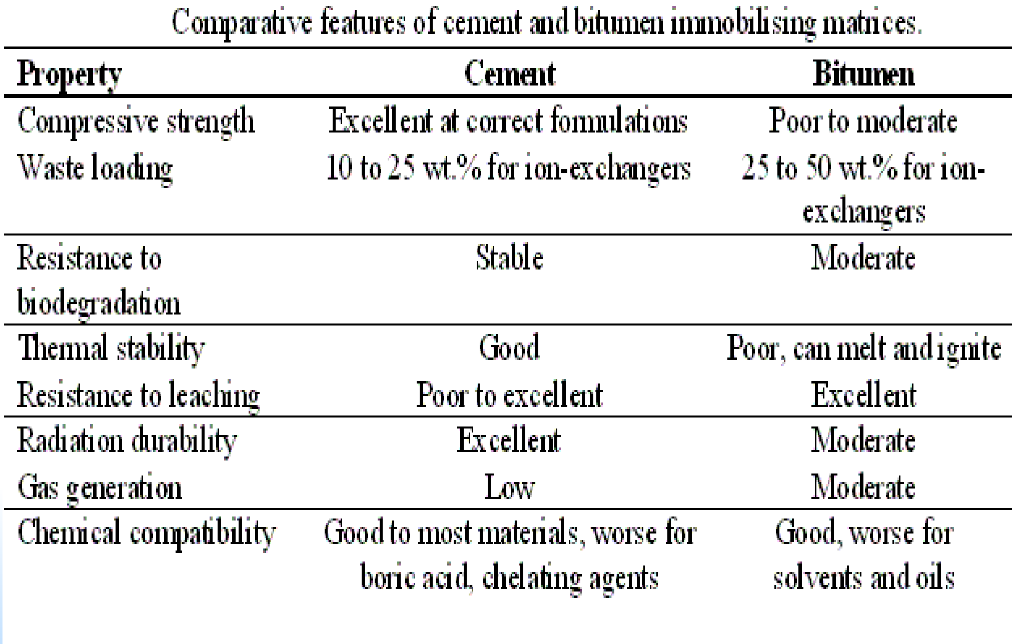

Comparative features of cement and bitumen immobilising matrices.

Property	Cement	Bitumen
Compressive strength	Excellent at correct formulations	Poor to moderate
Waste loading	10 to 25 wt.% for ion-exchangers	25 to 50 wt.% for ion-exchangers
Resistance to biodegradation	Stable	Moderate
Thermal stability	Good	Poor, can melt and ignite
Resistance to leaching	Poor to excellent	Excellent
Radiation durability	Excellent	Moderate
Gas generation	Low	Moderate
Chemical compatibility	Good to most materials, worse for boric acid, chelating agents	Good, worse for solvents and oils

Disadvantages:

- **Combustible material, although not easily flammable**
- **Lower stability against radiation than cement;**
- **Reacting with oxidizing materials such as sodium nitrate.**

Core samples from the natural **Oklo Reactor** have inclusion containing bitumen, that depressed the oxidative dissolution of the uraninite cores.

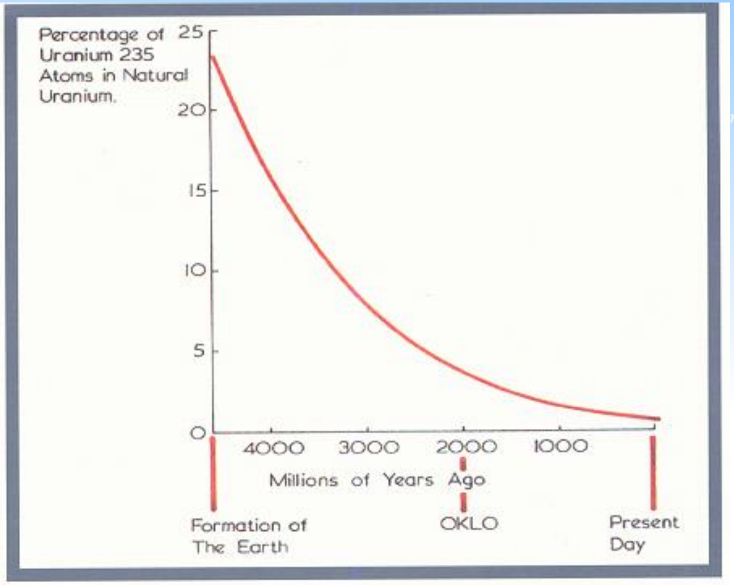

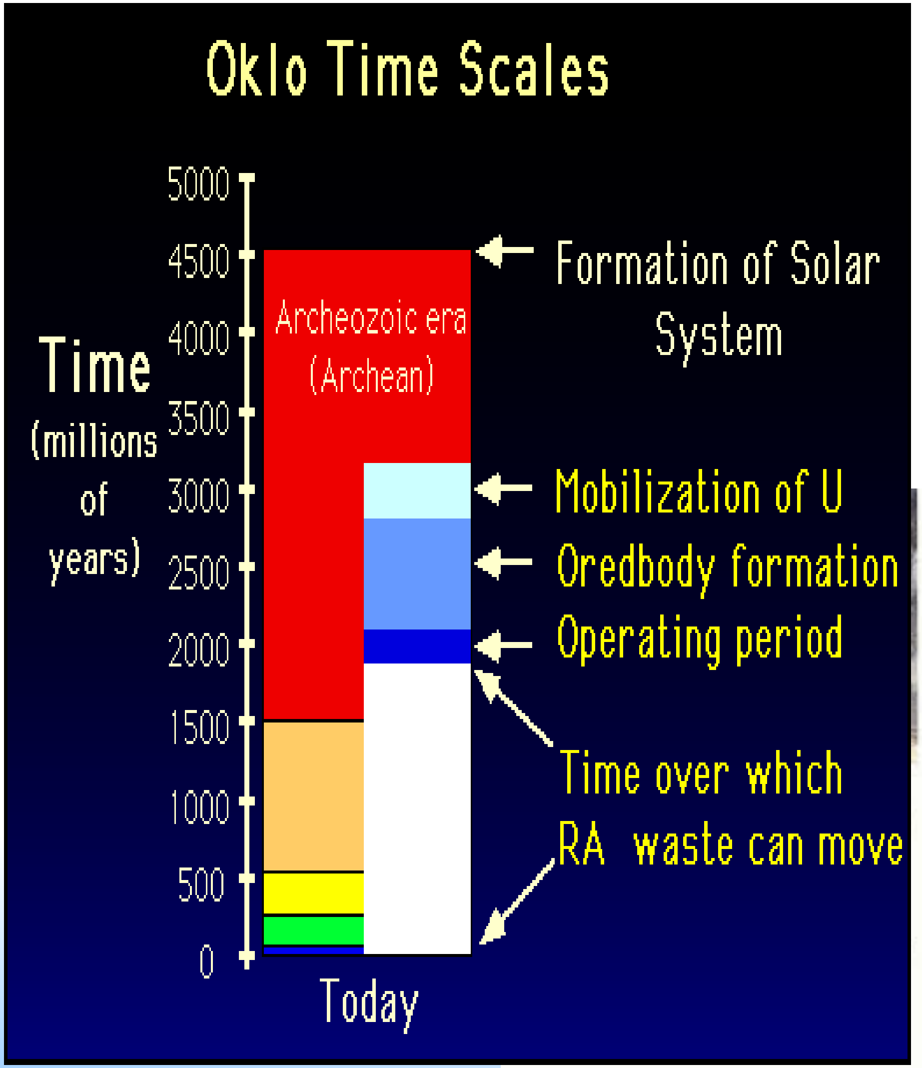

15 natural nuclear reactors operated for several millions years.

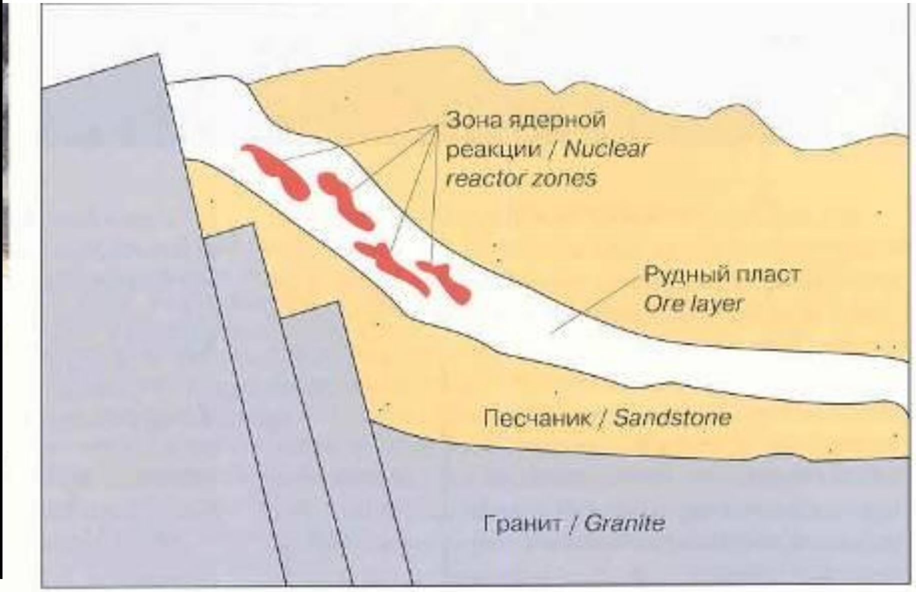

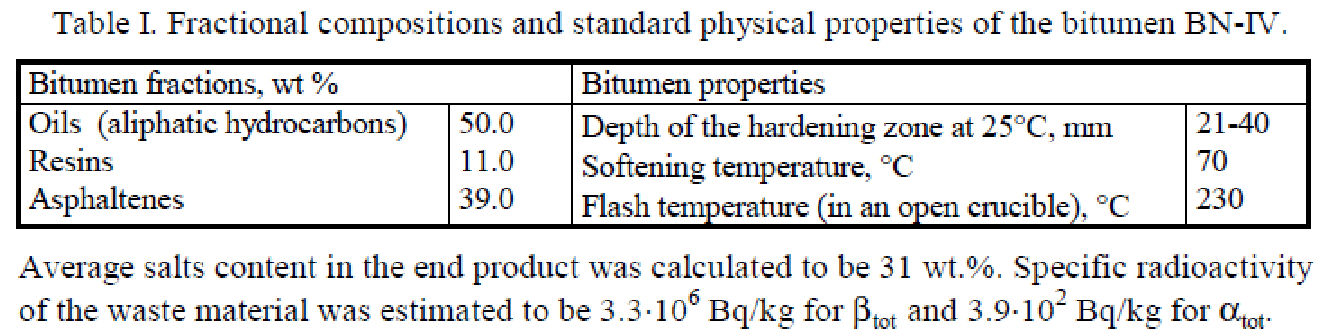

Table I. Fractional compositions and standard physical properties of the bitumen BN-IV.

Bitumen fractions, wt %		Bitumen properties	
Oils (aliphatic hydrocarbons)	50.0	Depth of the hardening zone at 25°C, mm	21-40
Resins	11.0	Softening temperature, °C	70
Asphaltenes	39.0	Flash temperature (in an open crucible), °C	230

Average salts content in the end product was calculated to be 31 wt.%. Specific radioactivity of the waste material was estimated to be $3.3 \cdot 10^6$ Bq/kg for β_{tot} and $3.9 \cdot 10^2$ Bq/kg for α_{tot}.

Bituminous materials consist of Hydrocarbons: (1) Asphaltenes, (2) Resins, and (3) Oils (aliphatic hydrocarbons).

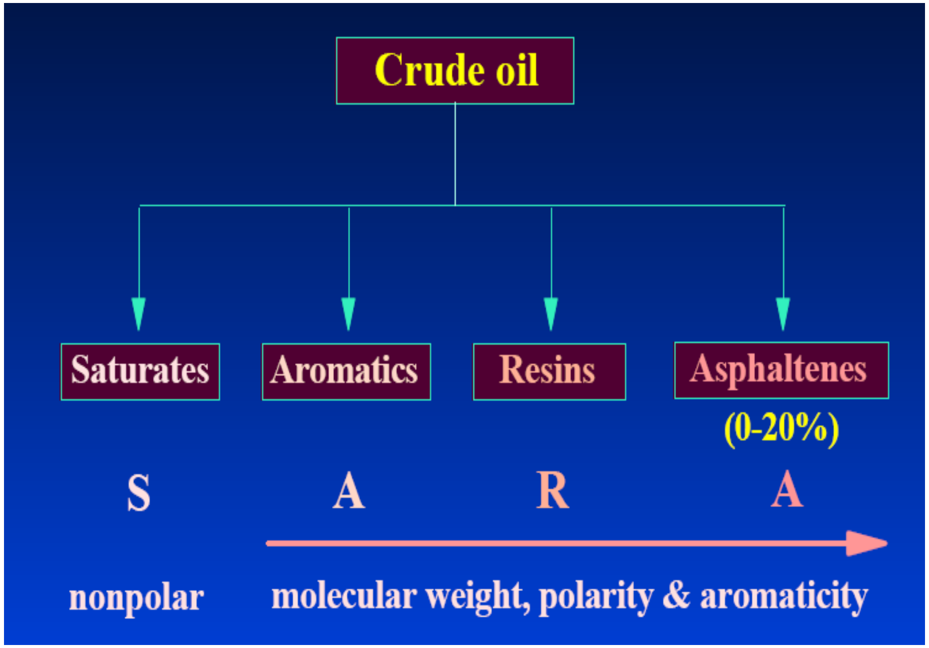

Crude oil

Saturates **Aromatics** **Resins** **Asphaltenes**

(0-20%)

S A R A

nonpolar

molecular weight, polarity & aromaticity

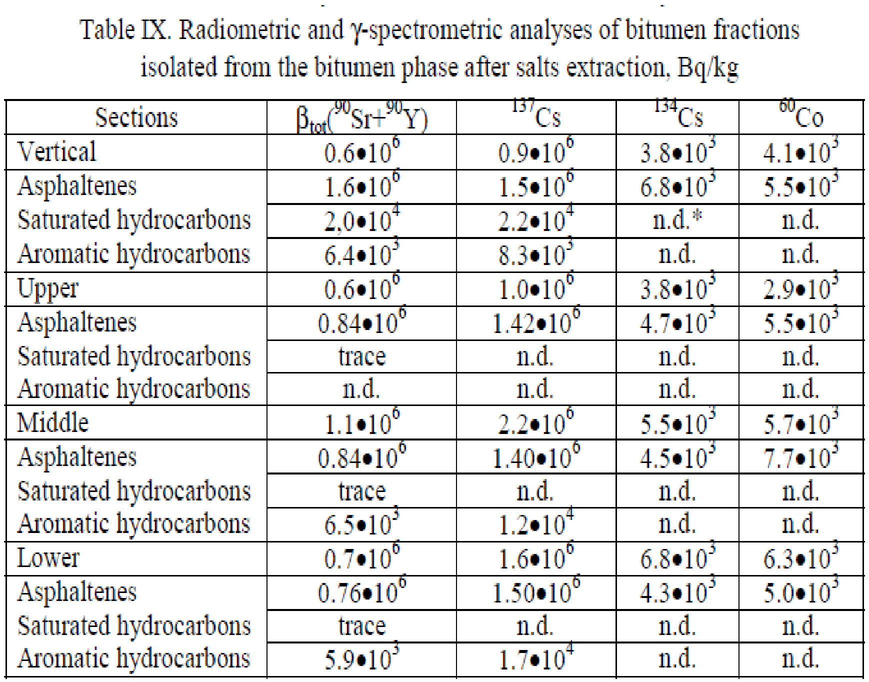

Table IX. Radiometric and γ-spectrometric analyses of bitumen fractions isolated from the bitumen phase after salts extraction, Bq/kg

Sections	$\beta_{tot}(^{90}Sr+^{90}Y)$	^{137}Cs	^{134}Cs	^{60}Co
Vertical	$0.6 \bullet 10^6$	$0.9 \bullet 10^6$	$3.8 \bullet 10^3$	$4.1 \bullet 10^3$
Asphaltenes	$1.6 \bullet 10^6$	$1.5 \bullet 10^6$	$6.8 \bullet 10^3$	$5.5 \bullet 10^3$
Saturated hydrocarbons	$2{,}0 \bullet 10^4$	$2.2 \bullet 10^4$	n.d.*	n.d.
Aromatic hydrocarbons	$6.4 \bullet 10^3$	$8.3 \bullet 10^3$	n.d.	n.d.
Upper	$0.6 \bullet 10^6$	$1.0 \bullet 10^6$	$3.8 \bullet 10^3$	$2.9 \bullet 10^3$
Asphaltenes	$0.84 \bullet 10^6$	$1.42 \bullet 10^6$	$4.7 \bullet 10^3$	$5.5 \bullet 10^3$
Saturated hydrocarbons	trace	n.d.	n.d.	n.d.
Aromatic hydrocarbons	n.d.	n.d.	n.d.	n.d.
Middle	$1.1 \bullet 10^6$	$2.2 \bullet 10^6$	$5.5 \bullet 10^3$	$5.7 \bullet 10^3$
Asphaltenes	$0.84 \bullet 10^6$	$1.40 \bullet 10^6$	$4.5 \bullet 10^3$	$7.7 \bullet 10^3$
Saturated hydrocarbons	trace	n.d.	n.d.	n.d.
Aromatic hydrocarbons	$6.5 \bullet 10^3$	$1.2 \bullet 10^4$	n.d.	n.d.
Lower	$0.7 \bullet 10^6$	$1.6 \bullet 10^6$	$6.8 \bullet 10^3$	$6.3 \bullet 10^3$
Asphaltenes	$0.76 \bullet 10^6$	$1.50 \bullet 10^6$	$4.3 \bullet 10^3$	$5.0 \bullet 10^3$
Saturated hydrocarbons	trace	n.d.	n.d.	n.d.
Aromatic hydrocarbons	$5.9 \bullet 10^3$	$1.7 \bullet 10^4$	n.d.	n.d.

Heavy-weight fractions of bitumen, e.g. asphaltenes impart viscoelastic properties to bitumen at ambient temperatures (10-40°C). Light-weight fractions, e.g. oils act as a carrier for the asphaltenes and resins.

Radiation effects in bitumen

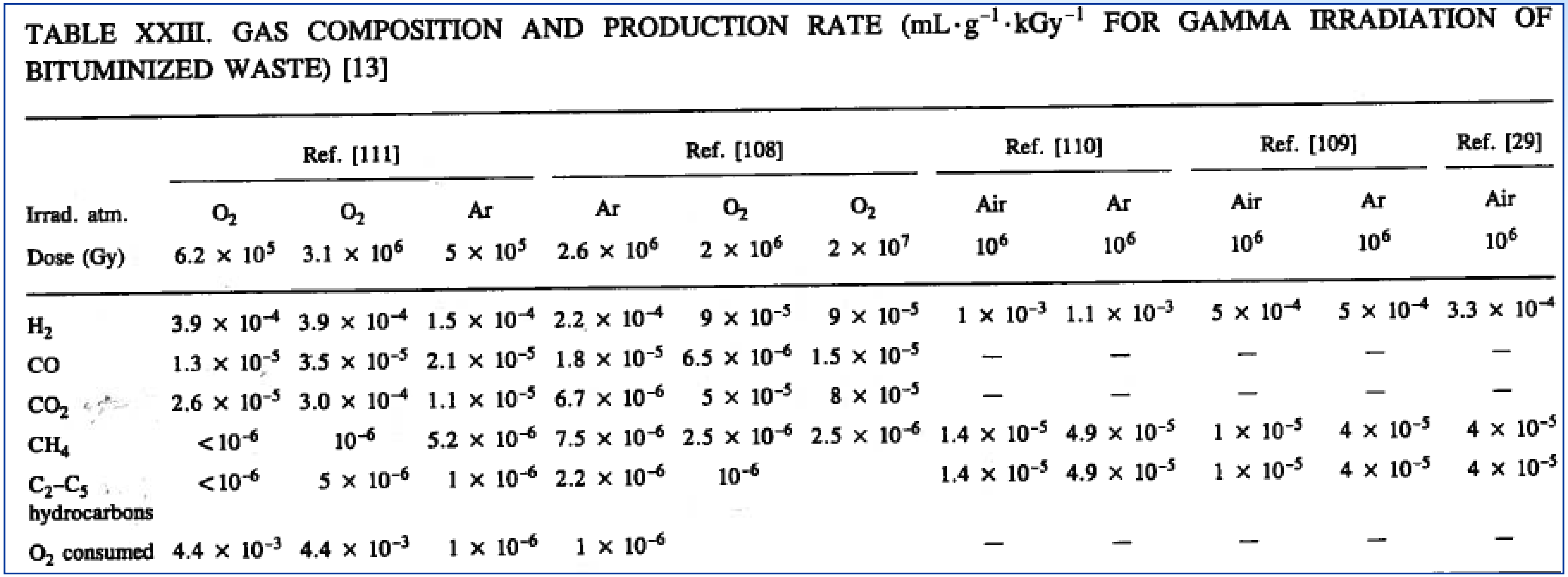

TABLE XXIII. GAS COMPOSITION AND PRODUCTION RATE ($mL \cdot g^{-1} \cdot kGy^{-1}$ FOR GAMMA IRRADIATION OF BITUMINIZED WASTE) [13]

	Ref. [111]			Ref. [108]			Ref. [110]		Ref. [109]		Ref. [29]
Irrad. atm.	O_2	O_2	Ar	Ar	O_2	O_2	Air	Ar	Air	Ar	Air
Dose (Gy)	6.2×10^5	3.1×10^6	5×10^5	2.6×10^6	2×10^6	2×10^7	10^6	10^6	10^6	10^6	10^6
H_2	3.9×10^{-4}	3.9×10^{-4}	1.5×10^{-4}	2.2×10^{-4}	9×10^{-5}	9×10^{-5}	1×10^{-3}	1.1×10^{-3}	5×10^{-4}	5×10^{-4}	3.3×10^{-4}
CO	1.3×10^{-5}	3.5×10^{-5}	2.1×10^{-5}	1.8×10^{-5}	6.5×10^{-6}	1.5×10^{-5}	—	—	—	—	—
CO_2	2.6×10^{-5}	3.0×10^{-4}	1.1×10^{-5}	6.7×10^{-6}	5×10^{-5}	8×10^{-5}	—	—	—	—	—
CH_4	$< 10^{-6}$	10^{-6}	5.2×10^{-6}	7.5×10^{-6}	2.5×10^{-6}	2.5×10^{-6}	1.4×10^{-5}	4.9×10^{-5}	1×10^{-5}	4×10^{-5}	4×10^{-5}
C_2–C_5 hydrocarbons	$< 10^{-6}$	5×10^{-6}	1×10^{-6}	2.2×10^{-6}	10^{-6}		1.4×10^{-5}	4.9×10^{-5}	1×10^{-5}	4×10^{-5}	4×10^{-5}
O_2 consumed	4.4×10^{-3}	4.4×10^{-3}	1×10^{-6}	1×10^{-6}			—	—	—	—	—

Radiation durability of BWP is > 0.5 to 2 MGy above which significant (>3%) swelling occurs. Hydrogen is the main radiolysis product.

The G-values for radiolytic hydrogen production are from 0.2 to 0.4 (compare it with G_{OH} = 2.8 of water exposed to gamma radiation).

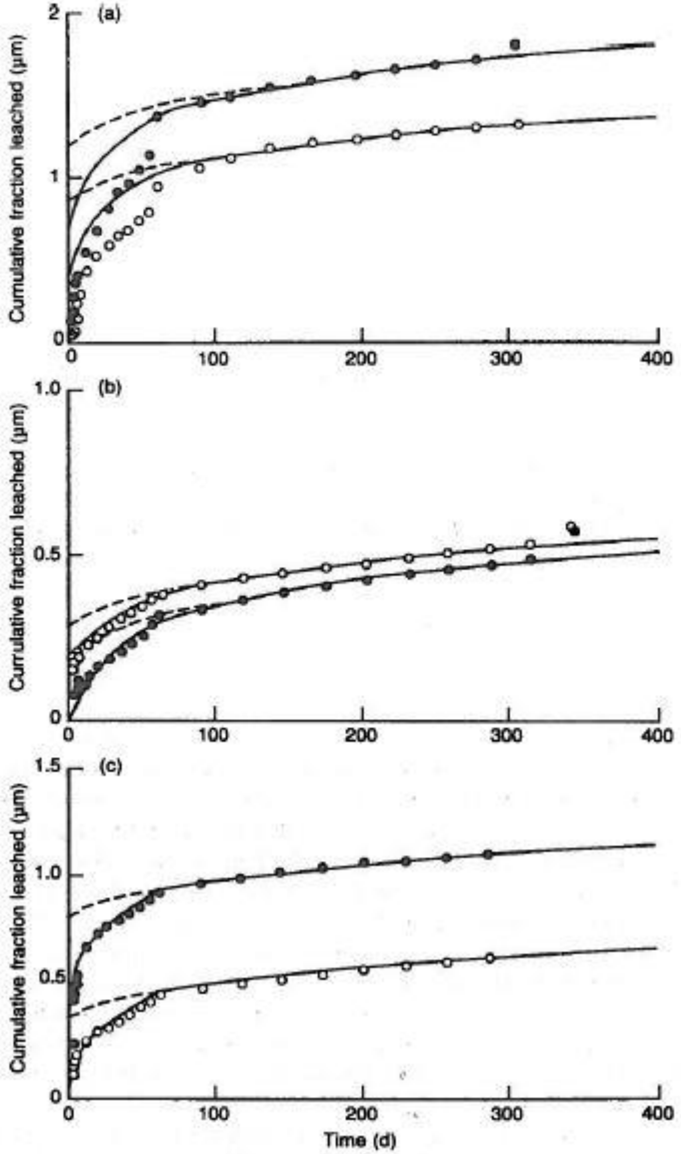

FIG. 15. Cumulative ^{137}Cs fraction leached from RWF7, unirradiated (a), and irradiated to 1 MGy (b) and 10 MGy (c) (RWF7: reprocessing waste concentrate incorporated into blown bitumen R85/40) [110]. The curves are for: ——, diffusion + sorption model; - - - -, diffusion model. The data (●, ○) are for duplicate models.

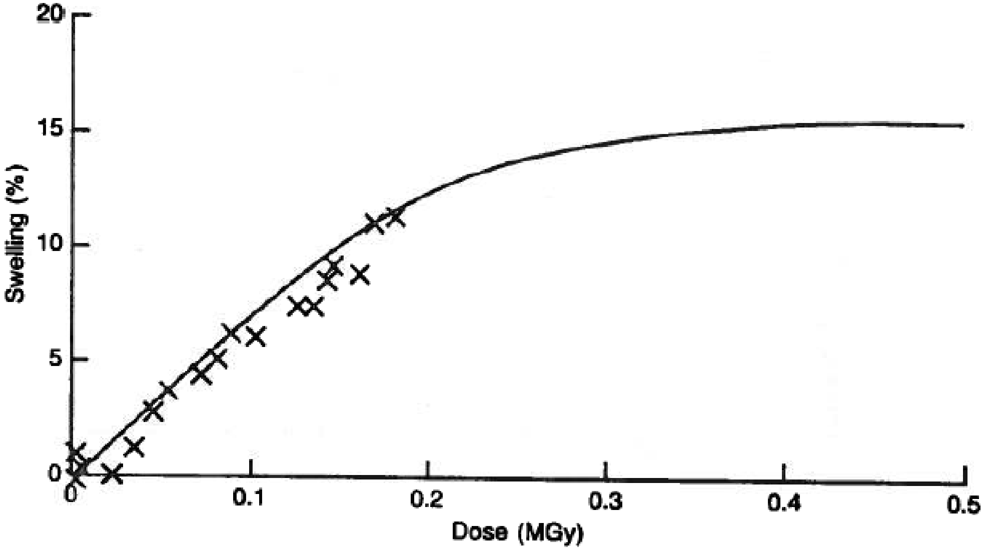

IG. 14. Comparison of experimental data on swelling taken over six years (×) with model redictions (curve) for a full size drum containing bituminized reprocessing waste sludges from a Hague: 11.5 TBq (312 Ci), β–γ; 30 GBq (0.8 Ci), α; product viscosity, 1 MPa s; gas roduction, 0.6 L·kg^{-1}·MGy^{-1} [25].

Leaching behaviour of BWP is little affected by irradiation.

In general releases are controlled by diffusion.

Bituminised waste products (BWP) leaching behaviour

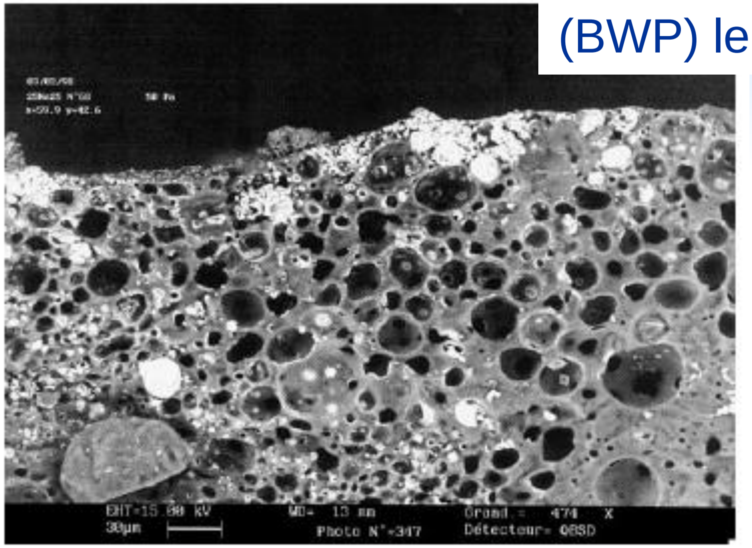

Fig. 2. ESEM observation of a leached synthetic BW showing the typical aspect of the permeable layer (bubbles filled with a saline solution).

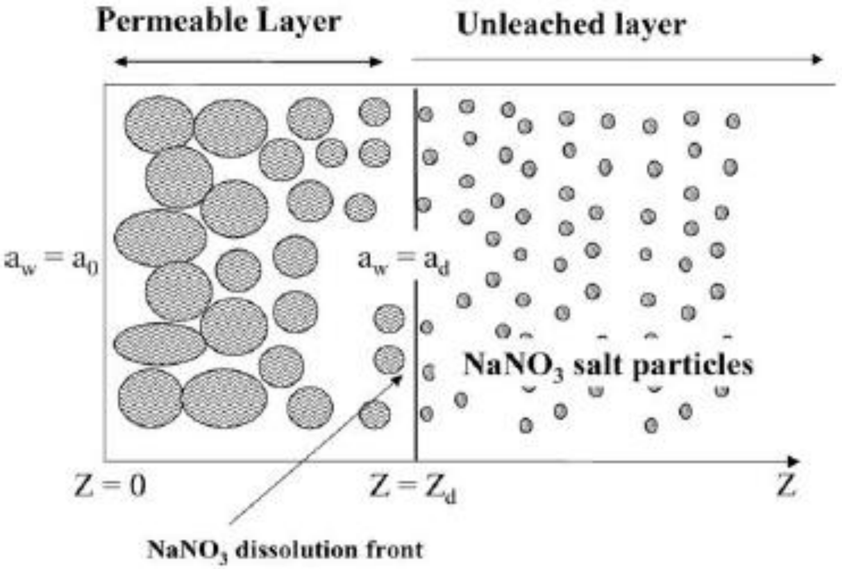

ied BW with the *Z*

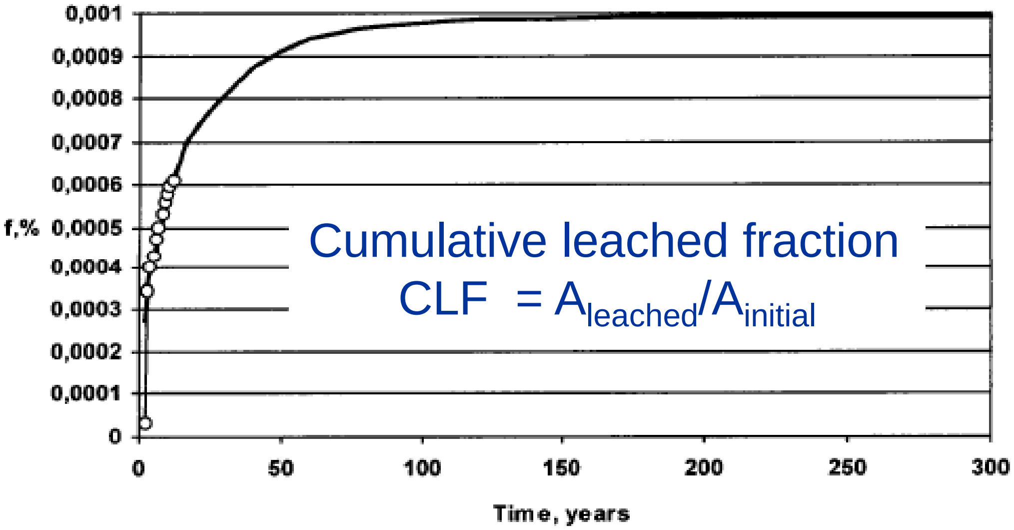

Cumulative leached fraction

CLF $= A_{leached}/A_{initial}$

Fig.2. The leached radioactivity fraction of a block of bituminized radioactive waste (f_l).

Percolation effects in bituminised waste products (BWP) leaching behaviour with waste loading

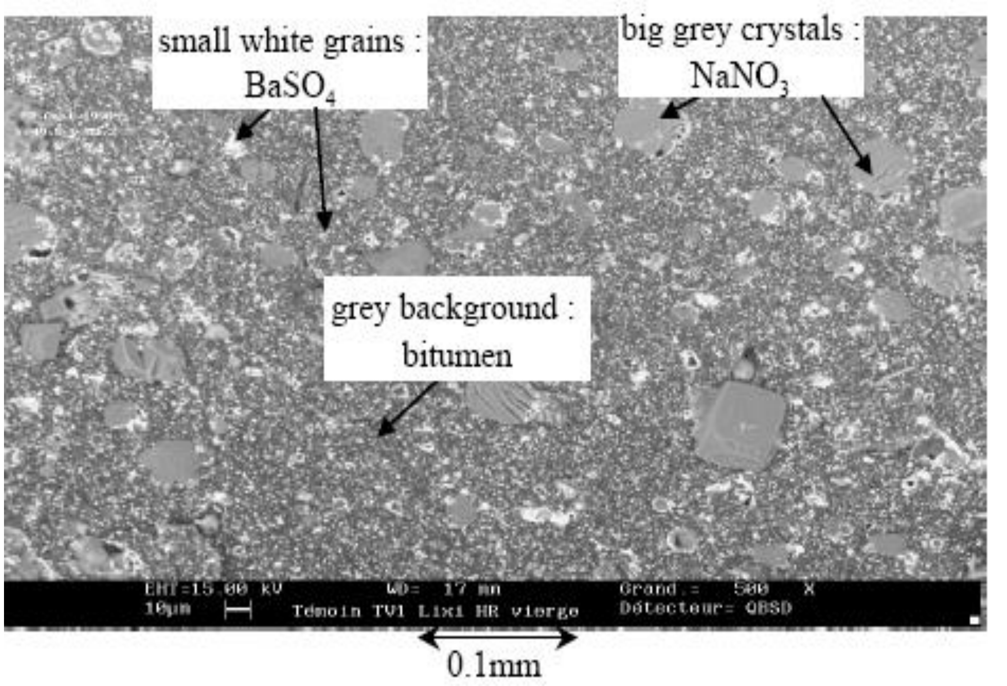

Scanning electronic microscope view of a synthetic bituminized waste reveals the presence of large (20-50 µm) $NaNO_3$ crystals and small (~1 µm) $BaSO_4$ crystals.

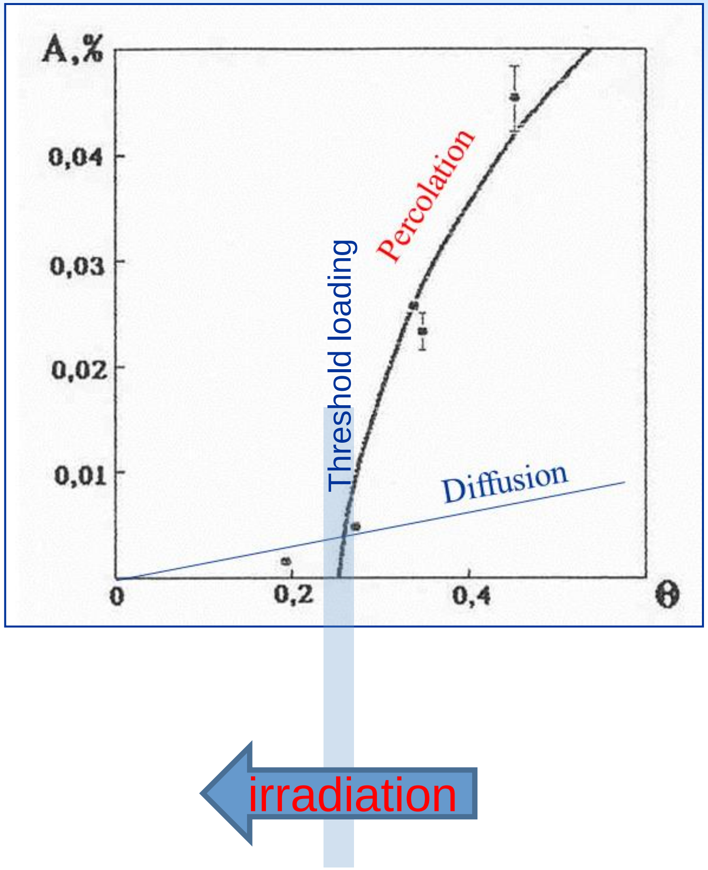

Essentially all radioactivity of the bitumen is associated with the asphaltene fraction. Aging of the bitumen wasteform leads to an increase in asphaltene fraction content and hardening of the bitumen matrix.

Conclusions on bitumen

Parameter	Value
Chemical durability (leaching rate Cs-137), g/cm^2 day, less than	1 10^{-3}
Stability to swelling (volume increase after 90-day immersion in water), %, less than	3
Content of free water:	
For salt concentrates, %, less than:	1
For ion-exchange resins, %	3 - 5
Thermal durability:	
Flash point, ^{o}C, not below	200
Ignition temperature, ^{o}C, not below	250
Self-ignition temperature, ^{o}C, not below:	400
Radiation durability, increase of volume after **10^6 Gy**, vol% not above	3
Biological stability	Absence of fungus

- Radiation durability of BWP is not high and is typically about 1 MGy.

The main effects of irradiation are radiolysis gas releases which finally cause swelling of wasteform, and ageing effects which gradually lead to bitumen hardening.

References:

1. M.I. Ojovan, W.E. Lee. An Introduction to Nuclear Waste Immobilisation, 2nd Edition, Elsevier, Amsterdam, 362 p. (2014).
2. J. Sercombe, B. Gwinner, C. Tiffreau, B. Simondi-Teisseire, F. Adenot. Modelling of bituminized radioactive waste leaching. Part I: Constitutive equations. *J. Nucl. Mater.* **349** 96–106 (2006).
3. M.I. Ojovan, N.V. Ojovan, Z.I. Golubeva., I.V. Startceva, A.S. Barinov. Aging of the bitumen waste form in wet repository conditions. *Mat. Res. Soc. Symp. Proc.*, **713**, 713-718 (2002).
4. K.P. Zakharova, O.L. Masanov. Bituminization of liquid radioactive wastes. Safety assessment and operational experience. *At. Energy*, **89**, 135-139 (2000).
5. IAEA TRS 352. Bituminization processes to condition radioactive wastes. IAEA, Vienna (1993).

IAEA

60 Years

Atoms for Peace and Development

Thank you!